

Choosing a basis that eliminates spurious solutions in $\mathbf{k} \cdot \mathbf{p}$ theory

Bradley A. Foreman*

Department of Physics, Hong Kong University of Science and Technology, Clear Water Bay, Kowloon, Hong Kong, China

A small change of basis in $\mathbf{k} \cdot \mathbf{p}$ theory yields a Kane-like Hamiltonian for the conduction and valence bands of narrow-gap semiconductors that has no spurious solutions, yet provides an accurate fit to all effective masses. The theory is shown to work in superlattices by direct comparison with first-principles density-functional calculations of the valence subband structure. A reinterpretation of the standard data-fitting procedures used in $\mathbf{k} \cdot \mathbf{p}$ theory is also proposed.

PACS numbers: 73.21.-b, 73.61.Ey, 71.15.Ap, 71.20.Nr

I. INTRODUCTION

The Kane model for coupled conduction and valence electrons in narrow-gap bulk semiconductors^{1,2,3} was first applied to superlattices three decades ago.⁴ Today this model is still used frequently for the study of medium- and narrow-gap nanostructures.^{5,6,7,8,9,10,11,12,13} Kane's theory has a notorious pitfall: spurious solutions with large crystal momentum \mathbf{k} , which arise from small Hamiltonian matrix elements of order k^2 .^{14,15,16,17,18,19,20,21,22,23,24,25,26,27,28,29,30,31,32,33,34,35,36,37,38,39,40,41,42,43,44,45,46,7,8,9,11,12,13,47} Spurious propagating waves pose a serious problem, since their presence within the energy gap changes the physical character of the model system from semiconducting to metallic.

Many schemes for eliminating the unphysical effects of spurious solutions have been proposed (e.g., changing or adding parameters in the Hamiltonian, or excising the offending modes numerically or analytically), but none has yet found wide acceptance. The relative merits of the various proposals are not discussed here. Instead, it is merely noted that all of these schemes take the form of patches applied to Kane's original $\mathbf{k} \cdot \mathbf{p}$ theory. The possibility of reconstructing $\mathbf{k} \cdot \mathbf{p}$ theory on a different foundation has not been considered.

This paper derives from first principles an 8×8 $\mathbf{k} \cdot \mathbf{p}$ Hamiltonian with no spurious solutions. The key step is a slight change in the standard choice of basis. This allows the adjustment-of-parameters method of Ref. 32, which was proposed only as a useful approximation, to be formulated rigorously. The present derivation proves that—within the limitations imposed by a second-order differential equation—*this method is not an approximation*. That is, all terms of order k^2 derived from a clearly defined basis can be included without approximation. (The number of fitting parameters can be reduced with a few standard approximations,^{2,32,48} but that is not a fundamental limitation of the method.) The change of basis is applied here to the first-principles envelope-function theory developed in Refs. 49, 50, and 51. A comparison with density-functional calculations on $\text{In}_{0.53}\text{Ga}_{0.47}\text{As}/\text{InP}$ superlattices shows very good agreement.

In conventional $\mathbf{k} \cdot \mathbf{p}$ perturbation theory,^{52,53} one uses a unitary transformation to construct a basis in which the $\mathbf{k} \cdot \mathbf{p}$ coupling between the states of interest (set \mathcal{A})

and all other states (set \mathcal{B}) is reduced to zero, while simultaneously renormalizing the masses in \mathcal{A} and \mathcal{B} . If \mathcal{A} includes the highest valence and lowest conduction states, the $\mathbf{k} \cdot \mathbf{p}$ coupling within \mathcal{A} is either set to zero (in single-band effective-mass theory^{3,52}) or not modified at all (in the multiband Kane theory^{2,3,53}).

In the present approach, a unitary transformation is used to modify the conduction–valence $\mathbf{k} \cdot \mathbf{p}$ interaction by only a small amount. The coupling can be either strengthened or weakened; its actual value is fixed (in one of several possible choices) by setting the partially renormalized conduction-band mass to zero. This is precisely the method used to eliminate spurious solutions in Ref. 32. However, the interface operator ordering derived here is more subtle than the simple heuristic model of Ref. 32. The present theory also suggests the need for a reinterpretation of the standard data-fitting procedures used in $\mathbf{k} \cdot \mathbf{p}$ models.

The situation encountered here is analogous to a gauge transformation in quantum electrodynamics. Although all gauges are equivalent in exact calculations, different gauges may yield different predictions in approximate calculations.⁵⁴ Likewise, the unitary transformation defined here would have no effect in an exact calculation, but in a second-order $\mathbf{k} \cdot \mathbf{p}$ Hamiltonian of finite dimension, varying the parameters of the unitary transformation generates a metal-insulator phase transition in the model system. The remedy proposed here is simply to choose transformation parameters that lie within the physical (i.e., insulating) regime of the phase diagram.

The paper begins in Sec. II with the definition and application of the unitary transformation to bulk semiconductors. The theory is extended to heterostructures in Sec. III and applied to the widely used Pidgeon–Brown Hamiltonian⁴⁸ in Sec. IV. Numerical applications of the theory are presented in Sec. V. Finally, the results of the paper are summarized and discussed in Sec. VI.

II. BULK CRYSTALS

A. Hamiltonian

Consider first the case of a bulk semiconductor. It is assumed at the outset that a Luttinger–Kohn (LK) uni-

tary transformation^{52,53} has already been used to eliminate the $\mathbf{k} \cdot \mathbf{p}$ coupling between sets \mathcal{A} and \mathcal{B} . Thus, the effective Hamiltonian H for states in \mathcal{A} is (in the LK basis)

$$\langle n\mathbf{k}|H|n'\mathbf{k}'\rangle = H_{nn'}(\mathbf{k})\delta_{\mathbf{k}\mathbf{k}'}, \quad (1a)$$

$$H_{nn'}(\mathbf{k}) = E_n\delta_{nn'} + k_i\pi_{nn'}^i + k_ik_jD_{nn'}^{ij}, \quad (1b)$$

in which E_n is the energy of state n at $\mathbf{k} = \mathbf{0}$, $\pi_{nn'}^i$ is the i component of the kinetic momentum matrix, and $D_{nn'}^{ij}$ is the inverse effective-mass tensor (in atomic units)

$$D_{nn'}^{ij} = \frac{1}{2}(\delta_{ij}\delta_{nn'} + i\epsilon_{ijk}\sigma_{nn'}^k) + \frac{1}{2}\sum_l^{\mathcal{B}}\left(\frac{\pi_{nl}^i\pi_{ln'}^j}{\omega_{nl}} + \frac{\pi_{nl}^j\pi_{ln'}^i}{\omega_{n'l}}\right), \quad (2)$$

where $\omega_{nl} = E_n - E_l$. Here and below all equations are written (for simplicity) as if the potential energy were local, although a nonlocal pseudopotential was used for the numerical calculations in Sec. V. The term $\sigma_{nn'}^k$ is a matrix element of the Pauli spin operator, which accounts for the intrinsic magnetic dipole moment of the electron.⁵⁵

In Ref. 32, it was assumed to be permissible to treat $\pi_{nn'}^i$ as an adjustable parameter in Eq. (1). In this approach, $\pi_{nn'}^i$ is replaced by $\bar{\pi}_{nn'}^i = \pi_{nn'}^i + \Delta\pi_{nn'}^i$, in which $\Delta\pi_{nn'}^i$ has the same symmetry as $\pi_{nn'}^i$ and vanishes when $E_n = E_{n'}$, but is otherwise arbitrary. The Hamiltonian (1b) is then replaced by

$$\bar{H}_{nn'}(\mathbf{k}) = E_n\delta_{nn'} + k_i\bar{\pi}_{nn'}^i + k_ik_j\bar{D}_{nn'}^{ij}, \quad (3)$$

in which the matrix $\bar{D}_{nn'}^{ij}$ is adjusted to maintain agreement with all experimental effective masses. This constraint does not, however, completely determine $\bar{D}_{nn'}^{ij}$.

To see this, consider applying Eq. (2) separately to set \mathcal{A} and to the subset $\mathcal{A}_{nn'} \subseteq \mathcal{A}$ defined by $\mathcal{A}_{nn'} = \{|n''\mathbf{k}\rangle \mid \min(E_n, E_{n'}) \leq E_{n''} \leq \max(E_n, E_{n'})\}$. A comparison of the results for \mathcal{A} and $\mathcal{A}_{nn'}$ gives

$$D_{nn'}^{ij}(\mathcal{A}_{nn'}) = D_{nn'}^{ij} + \frac{1}{2}\sum_l^{\mathcal{A}_{nn'}}\left(\frac{\pi_{nl}^i\pi_{ln'}^j}{\omega_{nl}} + \frac{\pi_{nl}^j\pi_{ln'}^i}{\omega_{n'l}}\right), \quad (4)$$

where $D_{nn'}^{ij} \equiv D_{nn'}^{ij}(\mathcal{A})$ and $\bar{\mathcal{A}}_{nn'} = \mathcal{A} \setminus \mathcal{A}_{nn'}$ is the complement of $\mathcal{A}_{nn'}$ in \mathcal{A} . When $E_n = E_{n'}$, $D_{nn'}^{ij}(\mathcal{A}_{nn'})$ is an experimentally measurable effective-mass parameter for the subspace $\mathcal{A}_{nn'}$.

If $\pi_{nn'}^i$ is treated as an adjustable parameter ($\pi_{nn'}^i \rightarrow \bar{\pi}_{nn'}^i$) and $D_{nn'}^{ij}(\mathcal{A}_{nn'})$ is assumed to be independent of $\{\Delta\pi_{nn'}^i\}$, then $\bar{D}_{nn'}^{ij}$ must satisfy

$$\bar{D}_{nn'}^{ij} \stackrel{?}{=} D_{nn'}^{ij}(\mathcal{A}_{nn'}) - \frac{1}{2}\sum_l^{\bar{\mathcal{A}}_{nn'}}\left(\frac{\bar{\pi}_{nl}^i\bar{\pi}_{ln'}^j}{\omega_{nl}} + \frac{\bar{\pi}_{nl}^j\bar{\pi}_{ln'}^i}{\omega_{n'l}}\right). \quad (5)$$

However, in general it is only necessary for Eq. (5) to be satisfied when $E_n = E_{n'}$. This still leaves some freedom of choice in the definition of $\bar{D}_{nn'}^{ij}$.

In this paper, the modified Hamiltonian (3) is derived by applying a unitary transformation e^S to the original Hamiltonian (1):

$$\bar{H} = e^{-S}He^S = H + [H, S] + \frac{1}{2!}[[H, S], S] + \dots, \quad (6)$$

where $S = -S^\dagger$ has matrix elements only within set \mathcal{A} . The generator S is defined by

$$\langle n\mathbf{k}|S|n'\mathbf{k}'\rangle = S_{nn'}(\mathbf{k})\delta_{\mathbf{k}\mathbf{k}'}, \quad (7a)$$

$$S_{nn'}(\mathbf{k}) = k_iS_{nn'}^i + k_ik_jS_{nn'}^{ij}, \quad (7b)$$

in which the linear coefficient is

$$S_{nn'}^i = \frac{\Delta\pi_{nn'}^i}{\omega_{nn'}}. \quad (8)$$

If $S_{nn'}^{ij} = 0$, the change $\Delta D_{nn'}^{ij} = \bar{D}_{nn'}^{ij} - D_{nn'}^{ij}$ is

$$\Delta D_{nn'}^{ij} = -\sum_l^{\mathcal{A}}\left(\frac{\Delta\pi_{nl}^i\bar{\pi}_{ln'}^j}{\omega_{nl}} + \frac{\bar{\pi}_{nl}^i\Delta\pi_{ln'}^j}{\omega_{n'l}}\right), \quad (9a)$$

in which $\bar{\pi}_{nn'}^i = \pi_{nn'}^i + \frac{1}{2}\Delta\pi_{nn'}^i$. Note that if we choose $\Delta\pi_{nn'}^i = -\pi_{nn'}^i$ (for $E_n \neq E_{n'}$), then $\bar{\pi}_{nn'}^i = 0$ and Eq. (9a) just adds extra terms to the summation in (2). Thus, if set \mathcal{A} comprises the highest valence and lowest conduction states, one-band effective-mass theory is given by $\Delta\pi_{nn'}^i = -\pi_{nn'}^i$, while the Kane model is given by $\Delta\pi_{nn'}^i = 0$. (See Appendix A for an alternative matrix formulation of this result.)

Equation (9a) can be rewritten as

$$\Delta D_{nn'}^{ij} = \frac{1}{2}\sum_l^{\mathcal{A}}(\pi_{nl}^i\pi_{ln'}^j - \bar{\pi}_{nl}^i\bar{\pi}_{ln'}^j)\left(\frac{1}{\omega_{nl}} + \frac{1}{\omega_{n'l}}\right) + \frac{\omega_{nn'}}{2}\sum_l^{\mathcal{A}}\frac{\Delta\pi_{nl}^i\pi_{ln'}^j - \pi_{nl}^i\Delta\pi_{ln'}^j}{\omega_{nl}\omega_{n'l}}, \quad (9b)$$

which shows that Eq. (5) is satisfied when $E_n = E_{n'}$, but not (in general) when $E_n \neq E_{n'}$. However, the degree of freedom corresponding to the coefficient $S_{nn'}^{ij}$ in Eq. (7) has not yet been used. Let

$$S_{nn'}^{ij} = \frac{\delta D_{nn'}^{ij}}{\omega_{nn'}}, \quad (10)$$

in which $\delta D_{nn'}^{ij}$ has the same symmetry as $D_{nn'}^{ij}$ and vanishes when $E_n = E_{n'}$, but is otherwise arbitrary. This has the effect of adding $\delta D_{nn'}^{ij}$ to the value of $\Delta D_{nn'}^{ij}$ given by Eq. (9). In this way, one can set the parameters $\bar{D}_{nn'}^{ij}$ for $E_n \neq E_{n'}$ to any desired value, including zero. This is merely a reflection of the fact that the terms $D_{nn'}^{ij}$ with $E_n \neq E_{n'}$ do not contribute to the single-band effective-mass Hamiltonian,³ since their contributions are of order k^3 or higher.

As a particular example, one could choose

$$\delta D_{nn'}^{ij} = \frac{1}{2} \sum_l^{A_{nn'}} (\bar{\pi}_{nl}^i \bar{\pi}_{ln'}^j - \pi_{nl}^i \pi_{ln'}^j) \left(\frac{1}{\omega_{nl}} + \frac{1}{\omega_{n'l}} \right) + \frac{\omega_{nn'}}{2} \sum_l^A \frac{\pi_{nl}^i \Delta \pi_{ln'}^j - \Delta \pi_{nl}^i \pi_{ln'}^j}{\omega_{nl} \omega_{n'l}}, \quad (11)$$

which would bring Eq. (9) into agreement with Eq. (5). However, including these terms would make subsequent analysis more complicated, so for simplicity the choice $\delta D_{nn'}^{ij} = 0$ is adopted in the remainder of this paper. This choice makes little practical difference, since Eq. (11) is in fact zero in the Kane model when spin-orbit coupling is neglected in the momentum matrix,^{1,2,3,48} which is the only example treated explicitly here.

B. Definition and elimination of spurious solutions

The preceding theory can now be used to define spurious solutions precisely. Spurious solutions are often defined as eigenstates of the $\mathbf{k} \cdot \mathbf{p}$ Hamiltonian with large wave vectors, but this definition is not completely satisfactory because spurious states are sometimes found well inside the first Brillouin zone.³² As emphasized by Bastard,^{21,24} more important than the magnitude of the wave vector is its *instability* with respect to small changes of the Hamiltonian parameters. The unitary transformation (6) allows such a change of parameters to be performed even when the $\mathbf{k} \cdot \mathbf{p}$ Hamiltonian is calculated directly from first principles.

Let the wave vector be $\mathbf{k} = \mathbf{k}_{\parallel} + \hat{\mathbf{n}} k_{\perp}$, where $\hat{\mathbf{n}} \cdot \hat{\mathbf{n}} = 1$, $\hat{\mathbf{n}} \cdot \mathbf{k}_{\parallel} = 0$, and $\hat{\mathbf{n}}$ and \mathbf{k}_{\parallel} are real. A spurious solution is defined here as a root $k_{\perp}(E, \mathbf{k}_{\parallel})$ of the secular equation

$$\det[\bar{H}(\mathbf{k}) - E] = \sum_{l=0}^{2N} c_l(E, \mathbf{k}_{\parallel}) k_{\perp}^l = 0 \quad (12)$$

that is an *unbounded* function of $\{\Delta \pi_{nn'}^i\}$ for small $\{\Delta \pi_{nn'}^i\}$ and \mathbf{k}_{\parallel} and for real E near the energy gap. (Here N is the dimension of set \mathcal{A} .) This definition does not encompass all possible types of spurious solutions (see, for example, those generated by Hamiltonian matrix elements of order k^4 in Sec. V and Ref. 51), but it does include those that can be treated effectively by the present unitary transformation.⁵⁶ This definition has the advantage of simplifying subsequent analysis because it focuses attention on the asymptotic properties of the secular equation at large k_{\perp} rather than the general properties of the secular equation at arbitrary k_{\perp} .

Within the stated limits, all coefficients c_l in the secular equation (12) are bounded (i.e., $|c_l| \lesssim 1$ in atomic units). The roots $k_{\perp}(E, \mathbf{k}_{\parallel})$ can therefore be unbounded only near $c_{2N} = 0$. For a given direction $\hat{\mathbf{n}}$, c_{2N} is just the product of eigenvalues $\bar{d}_{\nu}(\hat{\mathbf{n}})$ ($\nu = 1, 2, \dots, N$) of the matrix $\bar{D}(\hat{\mathbf{n}}) \equiv \hat{n}_i \hat{n}_j \bar{D}^{ij}$. Hence, as $\{\Delta \pi_{nn'}^i\}$ varies, the

spurious roots k_{\perp}^{SP} are unbounded near the zeros of $\bar{d}_{\nu}(\hat{\mathbf{n}})$, disappearing at $\bar{d}_{\nu}(\hat{\mathbf{n}}) = 0$ because the order of the secular equation is reduced. In typical cases (see Sec. IV E), k_{\perp}^{SP} changes from large real to large complex values (or vice versa) in the neighborhood of each singular point $\bar{d}_{\nu}(\hat{\mathbf{n}}) = 0$.

Unphysical metallic behavior can be avoided by choosing $\{\Delta \pi_{nn'}^i\}$ (or in general S) such that the spurious roots disappear. As shown below, in the Pidgeon–Brown model,⁴⁸ this can be achieved for all directions $\hat{\mathbf{n}}$ by setting the conduction-band mass parameter $\bar{A} = 0$, which is the choice used in Ref. 32. This choice may not work in all models, but one can also choose S such that $\text{Im}(k_{\perp}^{\text{SP}}) \neq 0$ for all $\hat{\mathbf{n}}$ (or more precisely such that $|\text{Im}(k_{\perp}^{\text{SP}})| > k_0 > 0$, where k_0 is some chosen value). The implementation of these choices is discussed in greater detail in Sec. IV C.

C. Velocity

Although the transformation (6) replaces $\boldsymbol{\pi}$ with $\bar{\boldsymbol{\pi}}$ in the Hamiltonian, it does not do so in the velocity $\mathbf{v} = -i[\mathbf{x}, H]$, where \mathbf{x} is the coordinate. As shown in Appendix B, the effective velocity $\bar{\mathbf{v}} = e^{-S} \mathbf{v} e^S$ for set \mathcal{A} is given to first order in k by an expression of the form (1a) with

$$\bar{v}_{nn'}^i(\mathbf{k}) = \pi_{nn'}^i + k_i \delta_{nn'} + k_j \sum_l^{\mathcal{B}} \left(\frac{\pi_{nl}^j \pi_{ln'}^i}{\omega_{nl}} + \frac{\pi_{nl}^i \pi_{ln'}^j}{\omega_{n'l}} \right) - k_j \sum_l^{\mathcal{A}} \left(\frac{\Delta \pi_{nl}^j \pi_{ln'}^i}{\omega_{nl}} + \frac{\pi_{nl}^i \Delta \pi_{ln'}^j}{\omega_{n'l}} \right). \quad (13)$$

This shows that $\bar{\mathbf{v}}_{nn'}(\mathbf{k}) \neq \nabla_{\mathbf{k}} \bar{H}_{nn'}(\mathbf{k})$ even to zeroth order in k . That is, the velocity to order k^0 is $\boldsymbol{\pi}$, not $\bar{\boldsymbol{\pi}}$, for both \mathbf{v} and $\bar{\mathbf{v}}$. In the special case $\Delta \pi_{nn'} = -\pi_{nn'}$, Eq. (13) is equivalent to the optical transition matrix element given in Eq. (19) of Ref. 57.

D. Implications for parameter fitting

The above results suggest the need for a reinterpretation of prior work on experimental fitting of $\mathbf{k} \cdot \mathbf{p}$ parameters. In a model with a complete set of $D_{nn'}^{ij}$ parameters, the empirical masses and Landé g factors are not sufficient to determine H ; in fact, for $E_n \neq E_{n'}$, $\pi_{nn'}^i$ is arbitrary. This indeterminacy could in principle be resolved by fitting \mathbf{v} to measured oscillator strengths, but this is not usually done because optical transition rates are considered to be less reliable than resonance frequencies. Instead, the most common procedure is to fix a few values of $D_{nn'}^{ij}$ by setting the contributions from \mathcal{B} to zero or some other convenient value (see, e.g., Refs. 48, 58, 59, and 60), thereby permitting a deterministic fit of $\pi_{nn'}^i$ from frequency data.

However, this procedure is nothing but the present transformation (albeit without explicit recognition that a change of basis is involved) with $\bar{D}_{nn'}^{ij}$ chosen for criteria other than the elimination of spurious solutions. The outcome of the fitting procedure is thus $\bar{\pi}$, not π (although typically $\bar{\pi} \approx \pi$). This shows that the production of spurious gap states by many $\mathbf{k} \cdot \mathbf{p}$ parameter sets is not purely a matter of experimental necessity but at least partially an artifact of choices made in simplifying the \bar{D} matrix. Fitting $\bar{D}_{nn'}^{ij}$ to nonparabolic effects⁶¹ fails to resolve the quandary because the $O(k^4)$ terms needed for a correct description of nonparabolicity have been omitted. [Including $O(k^4)$ terms in the experimental data fitting is also of no help because it merely shifts the indeterminacy to a larger set of parameters.] In the absence of direct measurements of π , it is not possible to distinguish π from $\bar{\pi}$ (i.e., to define unambiguously the original LK basis) without using a microscopic model to calculate some or all of the $\mathbf{k} \cdot \mathbf{p}$ parameters (see, e.g., Refs. 62 and 63). Of course, the results are then only as good as the chosen model.

III. HETEROSTRUCTURES

The next step is to extend this change of basis from bulk crystals to heterostructures. Here it is applied to the nonlinear response theory of Refs. 49, 50, and 51, in which the heterostructure is treated as a perturbation of some virtual bulk reference crystal. To first order, the effective \mathcal{A} Hamiltonian is $H = H^{(0)} + H^{(1)}$, where the reference Hamiltonian $H^{(0)}$ is handled according to the above methods, and the linear Hamiltonian $H^{(1)}$ is^{49,51}

$$\langle n\mathbf{k} | H^{(1)} | n'\mathbf{k}' \rangle = \sum_{\alpha} \theta_{\alpha}(\mathbf{k} - \mathbf{k}') H_{nn'}^{\alpha}(\mathbf{k}, \mathbf{k}'), \quad (14a)$$

where the sum covers independent values^{49,50} of α and

$$H_{nn'}^{\alpha}(\mathbf{k}, \mathbf{k}') = E_{nn'}^{\alpha} + \Xi^{\alpha} \delta_{nn'} \delta_{\mathbf{k}\mathbf{k}'} + k_i \pi_{nn'}^{i\alpha} + \pi_{nn'}^{\alpha i} k'_i + k_i k'_j D_{nn'}^{ij\alpha} + k_i D_{nn'}^{i\alpha j} k'_j + D_{nn'}^{\alpha ij} k'_i k'_j. \quad (14b)$$

Here $\theta_{\alpha}(\mathbf{k})$ is the Fourier transform of $\theta_{\alpha}(\mathbf{R})$, which is the change in fractional weight of atom α in cell \mathbf{R} of the heterostructure relative to the reference crystal. The coefficients in (14b) are defined in Ref. 51; they have the symmetry of site α in the reference crystal and satisfy hermiticity relations such as $D_{nn'}^{\alpha ij} = (D_{n'n}^{j\alpha i})^*$. The superscripts on these coefficients indicate how the coordinate and momentum operators are ordered. For example, in the coordinate representation, the term proportional to $D_{nn'}^{i\alpha j}$ has the BenDaniel–Duke ordering⁶⁴ $D_{nn'}^{i\alpha j} p_i \theta_{\alpha}(\mathbf{x}) p_j$, where \mathbf{p} is the momentum operator.⁶⁵ For a bulk perturbation of the form $\theta_{\alpha}(\mathbf{k} - \mathbf{k}') = \theta_{\alpha} \delta_{\mathbf{k}\mathbf{k}'}$, operator ordering is irrelevant and only the sums $\pi_{nn'}^{i\alpha} + \pi_{nn'}^{\alpha i}$ and $D_{nn'}^{ij\alpha} + D_{nn'}^{i\alpha j} + D_{nn'}^{\alpha ij}$ can be distinguished.

The unitary transformation (6) is now applied with $S = S^{(0)} + S^{(1)}$, where $S^{(0)}$ is the same as (7) and $S^{(1)}$

is defined by an expression similar to (14a) with

$$S_{nn'}^{\alpha}(\mathbf{k}, \mathbf{k}') = \frac{k_i \chi_{nn'}^{i\alpha} + \chi_{nn'}^{\alpha i} k'_i}{\omega_{nn'}}. \quad (15)$$

Here $\chi_{nn'}^{i\alpha}$ is only part of the change in $\pi_{nn'}^{i\alpha}$, since

$$\Delta \pi_{nn'}^{i\alpha} = \chi_{nn'}^{i\alpha} - \sum_l \frac{\Delta \pi_{nl}^i E_{ln'}^{\alpha}}{\omega_{nl}}, \quad (16a)$$

$$\Delta \pi_{nn'}^{\alpha i} = \chi_{nn'}^{\alpha i} - \sum_l \frac{E_{nl}^{\alpha} \Delta \pi_{ln'}^i}{\omega_{n'l}}, \quad (16b)$$

where $\Delta \pi_{nn'}^{\alpha i} = (\Delta \pi_{n'n}^{i\alpha})^*$. Likewise, the changes in the linear D tensor are given by

$$\Delta D_{nn'}^{ij\alpha} = - \sum_l \left(\frac{\Delta \pi_{nl}^i \tilde{\pi}_{ln'}^{j\alpha}}{\omega_{nl}} + \frac{\tilde{\pi}_{nl}^i \chi_{ln'}^{j\alpha}}{\omega_{n'l}} \right), \quad (17a)$$

$$\Delta D_{nn'}^{\alpha ij} = - \sum_l \left(\frac{\chi_{nl}^{\alpha i} \tilde{\pi}_{ln'}^j}{\omega_{nl}} + \frac{\tilde{\pi}_{nl}^{\alpha i} \Delta \pi_{ln'}^j}{\omega_{n'l}} \right), \quad (17b)$$

$$\Delta D_{nn'}^{i\alpha j} = - \sum_l \left(\frac{\Delta \pi_{nl}^i \tilde{\pi}_{ln'}^{\alpha j}}{\omega_{nl}} + \frac{\tilde{\pi}_{nl}^i \chi_{ln'}^{\alpha j}}{\omega_{n'l}} \right) - \sum_l \left(\frac{\chi_{nl}^{\alpha i} \tilde{\pi}_{ln'}^j}{\omega_{nl}} + \frac{\tilde{\pi}_{nl}^{\alpha i} \Delta \pi_{ln'}^j}{\omega_{n'l}} \right), \quad (17c)$$

where $\Delta D_{nn'}^{\alpha ij} = (\Delta D_{n'n}^{j\alpha i})^*$ and $\Delta D_{nn'}^{i\alpha j} = (\Delta D_{n'n}^{j\alpha i})^*$. This system of linear equations can be solved for $\Delta \pi^{\alpha}$ as a function of ΔD^{α} . An equivalent matrix formulation of Eqs. (16) and (17) is given in Appendix A.

IV. THE PIDGEON–BROWN MODEL

A. Conduction band

As an example, consider Pidgeon and Brown's formulation of the Kane model for a zinc-blende crystal.⁴⁸ The set $\mathcal{A} = \{\Gamma_{6c}, \Gamma_{8v}, \Gamma_{7v}\}$ is defined in the tensor-product basis $\{|S\rangle, |X\rangle, |Y\rangle, |Z\rangle\} \otimes \{|+\rangle, |-\rangle\}$, with spin-orbit coupling included only to order k^0 .^{1,2,3,48} For the bulk reference crystal, the relevant conduction-band (CB) constants are $A = D_{SS}^{xx}$ and $P = -i\pi_{SX}^x$. From Eqs. (4) and (9), the values of A and P are related to the CB effective mass m_c by

$$\frac{1}{2m_c} = A + \frac{P^2}{\epsilon_1} = \bar{A} + \frac{\bar{P}^2}{\epsilon_1}, \quad (18)$$

in which ϵ_n is the n^{th} -order reduced energy gap:

$$\frac{1}{(\epsilon_n)^n} = \frac{2}{3(E_g)^n} + \frac{1}{3(E_g + \Delta_{\text{so}})^n}, \quad (19)$$

where $E_g = E_{6c} - E_{8v}$ and $\Delta_{\text{so}} = E_{8v} - E_{7v}$. The value of $\bar{P} = -i\pi_{SX}^x$ needed to obtain a desired change $\Delta A = \bar{A} - A$ is therefore

$$\bar{P}^2 = P^2 - \epsilon_1 \Delta A. \quad (20)$$

The selection of suitable values of ΔA and \bar{P} is discussed below in Sec. IV C.

For the linear response in a heterostructure, there are two independent CB partial mass coefficients, $A^{\cdot\alpha} = A^{\alpha\cdot}$ and $A^{\alpha\cdot}$ (where $A^{\cdot\alpha} = D_{SS}^{x\alpha}$, $A^{\alpha\cdot} = D_{SS}^{\alpha xx}$, and $A^{\cdot\alpha} = D_{SS}^{x\alpha x}$), and two independent momentum parameters, $P^{\alpha\cdot} = -i\pi_{SX}^{\alpha x}$ and $P^{\cdot\alpha} = -i\pi_{SX}^{x\alpha}$. Upon solving Eqs. (16) and (17) for the changes $\Delta P^{\alpha\cdot}$ and $\Delta P^{\cdot\alpha}$ needed to obtain desired values of $\Delta A^{\cdot\alpha}$ and $\Delta A^{\alpha\cdot}$, one finds

$$\Delta P^{\alpha\cdot} = -\frac{\epsilon_1 \Delta A^{\alpha\cdot}}{\bar{P}} - \frac{P^{\alpha\cdot} \Delta P}{\bar{P}} - \frac{\epsilon_1^2 \Delta A E_c^\alpha}{2\epsilon_2^2 \bar{P}}, \quad (21a)$$

$$\Delta P^{\cdot\alpha} = -\frac{\epsilon_1 \Delta A^{\cdot\alpha}}{2\bar{P}} - \frac{P^{\cdot\alpha} \Delta P}{\bar{P}} + \frac{\epsilon_1^2 \Delta A E_v^\alpha}{2\epsilon_2^2 \bar{P}}, \quad (21b)$$

where $E_c^\alpha = E_{SS}^\alpha$ and

$$\frac{E_v^\alpha}{\epsilon_2^2} = \frac{2E_{8v}^\alpha}{3(E_g)^2} + \frac{E_{7v}^\alpha}{3(E_g + \Delta_{so})^2}. \quad (22)$$

If one adds (21a) and (21b) to obtain the total linear change $\Delta P^\alpha \equiv \Delta P^{\alpha\cdot} + \Delta P^{\cdot\alpha}$ for a bulk crystal, the result is identical to what is obtained from linear variation of the parameters in Eq. (20).

Equations (20) and (21) can now be inserted into (17) to determine the changes in the other mass parameters. The partially renormalized bulk CB Landé factor $g = -i2(D_{S+,S+}^{xy} - D_{S+,S+}^{yx})$ is related to the fully renormalized experimental value g_c by

$$g_c = g - \frac{4P^2}{3\delta_1} = \bar{g} - \frac{4\bar{P}^2}{3\delta_1}, \quad (23)$$

where

$$\frac{1}{(\delta_n)^n} = \frac{1}{(E_g)^n} - \frac{1}{(E_g + \Delta_{so})^n}. \quad (24)$$

The change $\Delta g = \bar{g} - g$ is therefore

$$\Delta g = -\frac{4\epsilon_1}{3\delta_1} \Delta A = -\left(\frac{4\Delta_{so}}{3E_g + 2\Delta_{so}}\right) \Delta A. \quad (25)$$

Likewise, the changes in the linear-response terms are

$$\Delta g^{\alpha\cdot} = -\frac{4\epsilon_1}{3\delta_1} \Delta A^{\alpha\cdot} - \frac{2}{3} \Delta A E_c^\alpha \left(\frac{\epsilon_1^2}{\delta_1 \epsilon_2^2} - \frac{\epsilon_1}{\delta_2^2} \right), \quad (26a)$$

$$\Delta g^{\cdot\alpha} = -\frac{4\epsilon_1}{3\delta_1} \Delta A^{\cdot\alpha} + \frac{4}{3} \Delta A \left(\frac{\epsilon_1^2 E_v^\alpha}{\delta_1 \epsilon_2^2} - \frac{\epsilon_1 \beta_v^\alpha}{\delta_2^2} \right), \quad (26b)$$

where

$$\frac{\beta_v^\alpha}{\delta_2^2} = \frac{E_{8v}^\alpha}{(E_g)^2} - \frac{E_{7v}^\alpha}{(E_g + \Delta_{so})^2}. \quad (27)$$

Note that $g^{\alpha\cdot}$ is also the linear contribution to the CB Rashba coefficient.⁵¹

When spin-orbit coupling is neglected in the remote \mathcal{B} states,^{1,2,3,48} one has simply $g = 2$.⁴⁸ In the original paper of Pidgeon and Brown,⁴⁸ the value of A was found

to have little effect on the calculated energy levels; therefore, it was treated as an adjustable parameter ($A \rightarrow \bar{A}$, $P \rightarrow \bar{P}$), with $\bar{A} = \frac{1}{2}$ chosen for simplicity. The Landé factor, however, was held fixed at $\bar{g} = 2$. The present results show that the assumption $\Delta g = 0$ must be regarded as an approximation because it cannot be reduced to a unitary transformation.

According to Eq. (25), Δg will be negligible in comparison to ΔA if the spin-orbit coupling is small ($\Delta_{so} \ll E_g$). However, the Pidgeon–Brown model is often used in cases where $\Delta_{so} \sim E_g$ or even $\Delta_{so} \gg E_g$. In such cases, setting $\Delta g = 0$ is no more justifiable than setting $\Delta A = 0$ when $\Delta P \neq 0$. But this problem is easily resolved by using the value (25) for Δg (assuming, of course, that the correct original value of A is known).

The Kane interband parameter $B = D_{SZ}^{xy} + D_{SZ}^{yx}$ is neglected in the Pidgeon–Brown model⁴⁸ because it corresponds to $O(k^3)$ terms in the single-band Hamiltonian. The value of B is not affected by the linear term $S_{nn'}^i$ in the generator (7) (i.e., $\Delta B = 0$) because B does not depend on P . Therefore, neglecting B is a consistent approximation in the sense that $B = 0$ implies $\bar{B} = 0$. Alternatively, one could choose $\delta D_{nn'}^{ij}$ in Eq. (10) to satisfy $\delta B = -B$, thus obtaining $\bar{B} = 0$ even when $B \neq 0$.

B. Valence band

1. Zero spin-orbit coupling

For the valence band, consider first the case without spin. There are four independent Γ_{15v} parameters:⁶⁶ $L = D_{XX}^{xx}$, $M = D_{XX}^{yy}$, $N = D_{XY}^{xy} + D_{XY}^{yx}$, and $K = D_{XY}^{xy} - D_{XY}^{yx}$. From Eqs. (4) and (9) we have

$$L^0 = L - P^2/E_g' = \bar{L} - \bar{P}^2/E_g', \quad (28a)$$

$$M^0 = M = \bar{M}, \quad (28b)$$

$$N^0 = N - P^2/E_g' = \bar{N} - \bar{P}^2/E_g', \quad (28c)$$

$$K^0 = K - P^2/E_g' = \bar{K} - \bar{P}^2/E_g', \quad (28d)$$

where [see Eq. (4)] $L^0 \equiv L(\mathcal{A}_0)$ is the parameter L evaluated for the subset $\mathcal{A}_0 = \{\Gamma_{15v}\}$, and $E_g' \equiv E_{1c} - E_{15v} = E_g + \frac{1}{3}\Delta_{so}$ is the energy gap in the absence of spin-orbit splitting. Under these conditions $\epsilon_1 = E_g'$, so the bulk changes are simply

$$\Delta L = \Delta N = \Delta K = -\Delta A, \quad \Delta M = 0. \quad (29)$$

Likewise, for the linear response, $\Delta M^{\alpha\cdot} = \Delta M^{\cdot\alpha} = 0$ and

$$\Delta L^{\alpha\cdot} = \Delta N^{\alpha\cdot} = \Delta K^{\alpha\cdot} = -\frac{1}{2} \Delta A^{\alpha\cdot}, \quad (30a)$$

$$\Delta L^{\cdot\alpha} = \Delta N^{\cdot\alpha} = \Delta K^{\cdot\alpha} = -2 \Delta A^{\cdot\alpha}. \quad (30b)$$

Again, the total bulk linear variation $\Delta L^\alpha \equiv \Delta L^{\cdot\alpha} + \Delta L^{\alpha\cdot} + \Delta L^{\alpha\cdot}$ is consistent with (29). However, the interchange of CB and VB operator orderings in (30)

is a new feature that was not predicted by the simple model of Ref. 32 (where only the numerical value of P was changed, and all terms with the ordering $X^{\alpha\cdots}$ were excluded⁶⁷).

Although it vanishes in bulk, the linear VB momentum does have one independent constant $R^\alpha = -i\pi_{XY}^{\alpha z}$ (with $R^\alpha \equiv -i\pi_{XY}^{\alpha z} = -R^\alpha$).⁵¹ This term is not affected by the change (16); i.e., $\Delta R^\alpha = \Delta R^\alpha = 0$.

2. Nonzero spin-orbit coupling

In the Kane model,^{1,2,3,48} spin-orbit coupling is included to order k^0 by adding the perturbation $H_{\text{so}} = \frac{1}{3}\Delta_{\text{so}}(\mathbf{I} \cdot \boldsymbol{\sigma})$ to the Hamiltonian for set $\mathcal{A} = \{\Gamma_{6c}, \Gamma_{8v}, \Gamma_{7v}\}$, where \mathbf{I} is the orbital angular momentum operator.⁶⁶ When working in a basis that diagonalizes H_{so} ,^{1,2,3,48} it is convenient to define the following linear transformation of the mass parameters:⁶⁶

$$\gamma_1 = -\frac{2}{3}(L + 2M), \quad L = -\frac{1}{2}(\gamma_1 + 4\gamma_2), \quad (31a)$$

$$\gamma_2 = -\frac{1}{3}(L - M), \quad M = -\frac{1}{2}(\gamma_1 - 2\gamma_2), \quad (31b)$$

$$\gamma_3 = -\frac{1}{3}N, \quad N = -3\gamma_3, \quad (31c)$$

$$\kappa = -\frac{1}{3}(K + 1), \quad K = -3\kappa - 1. \quad (31d)$$

Here γ_1 , γ_2 , γ_3 , and κ are the modified Luttinger parameters introduced by Pidgeon and Brown.⁴⁸ Upon applying Eq. (4) to the subset $\mathcal{A}_0 = \{\Gamma_{8v}\}$, one finds the relations⁴⁸

$$\gamma_1^0 = \gamma_1 + 2P^2/3E_g, \quad (32a)$$

$$\gamma_2^0 = \gamma_2 + P^2/3E_g, \quad (32b)$$

$$\gamma_3^0 = \gamma_3 + P^2/3E_g, \quad (32c)$$

$$\kappa^0 = \kappa + P^2/3E_g, \quad (32d)$$

where γ_1^0 , γ_2^0 , γ_3^0 , and κ^0 are the original Luttinger parameters⁶⁶ for Γ_{8v} . The Luttinger parameter $q^0 = q$ is neglected in the Kane model because (to leading order) it is proportional to the spin-orbit splitting of the remote \mathcal{B} states.⁶⁸ Since q is independent of P , it is not affected by the unitary transformation (6).

It is also convenient to introduce a linear transformation of the form (31) for the parameters γ_1^0 , γ_2^0 , γ_3^0 , and κ^0 in (32). When this is done, one finds that the parameters L^0 , M^0 , N^0 , and K^0 are related to L , M , N , and K by expressions similar to those given earlier in Eq. (28). The only difference is that the Γ_{15} energy gap E_g' is replaced [see Eq. (32)] by the Γ_8 gap E_g .

Now consider using Eq. (4) and (9) to determine how the effective-mass parameters change when the unitary transformation (6) is applied. For the Γ_{8v} submatrix, the results are similar to Eqs. (28) (with $E_g' \rightarrow E_g$) and (32):

$$Q_8^0 = Q_8 - P^2/E_g \quad (33a)$$

$$= \bar{Q}_8 - \bar{P}^2/E_g, \quad (33b)$$

where Q is any member of the set $\{L, N, K, -\frac{3}{2}\gamma_1, -3\gamma_2, -3\gamma_3, -3\kappa\}$ (M does not depend on P). The subscript 8 is added to emphasize that Eq. (33) holds for Γ_{8v} only. Here Q_8^0 is an original Luttinger parameter, while $Q_8 \equiv Q$ and \bar{Q}_8 are the modified Luttinger parameters before and after the unitary transformation.

However, when Eqs. (4) and (9) are applied to the Γ_{7v} submatrix, the results are different:

$$Q_7^0 = Q_7 - P^2/(E_g + \Delta_{\text{so}}) \quad (34a)$$

$$= \bar{Q}_7 - \bar{P}^2/(E_g + \Delta_{\text{so}}). \quad (34b)$$

In the Kane model, $Q_7 \equiv Q_8 \equiv Q$, but clearly $Q_7^0 \neq Q_8^0$ and (when $\bar{P}^2 \neq P^2$) $\bar{Q}_7 \neq \bar{Q}_8$. Such differences also occur in the $\Gamma_{7v} \times \Gamma_{8v}$ submatrix, where the parameters are given in terms of the above results by $Q_{78}^0 = \frac{1}{2}(Q_7^0 + Q_8^0)$, $Q_{78} = \frac{1}{2}(Q_7 + Q_8)$, and $\bar{Q}_{78} = \frac{1}{2}(\bar{Q}_7 + \bar{Q}_8)$. The changes in Q for each submatrix are therefore given by

$$\Delta Q_8 = -\frac{\epsilon_1 \Delta A}{E_g}, \quad \Delta Q_7 = -\frac{\epsilon_1 \Delta A}{E_g + \Delta_{\text{so}}},$$

$$\Delta Q_{78} = \frac{1}{2}(\Delta Q_7 + \Delta Q_8). \quad (35)$$

The result $Q_7^0 \neq Q_8^0$ merely reflects that the Luttinger parameters for Γ_{7v} are different from those for Γ_{8v} . (This fact is sometimes used to obtain an experimental fit for P .^{16,18,69}) However, the result $\Delta Q_7 \neq \Delta Q_8$ shows that the unitary transformation (6) does *not* preserve the initial equality of the modified Luttinger parameters in the Γ_{8v} , Γ_{7v} , and $\Gamma_{7v} \times \Gamma_{8v}$ submatrices.

The latter result is hardly surprising, because the modified Luttinger parameters are known to have different values in each submatrix when spin-orbit coupling is treated exactly.^{70,71,72} The inequality $\Delta Q_7 \neq \Delta Q_8$ is therefore nothing new from a physical standpoint. Nevertheless, it does serve to show that the standard experimental data-fitting procedure—namely, treating P as a fitting parameter and defining the modified Luttinger parameters for all of set \mathcal{A} from the Γ_{8v} Luttinger parameters via Eq. (32)—is *not* equivalent to a simple unitary transformation. Instead, as P is varied during the fitting, one must invoke the additional approximation of replacing ΔQ_7 with ΔQ_8 in order to preserve equality of the modified Luttinger parameters in all submatrices.

The assumption that the modified Luttinger parameters have the same value in all submatrices even when P is treated as a fitting parameter will be referred to as the Pidgeon–Brown approximation (PBA), since these authors seem to be the first to use it explicitly⁴⁸ (although this approximation is implicit in the theory of Kane^{1,2,3}). The validity of the PBA was studied by Boujdaria *et al.*,⁷³ who found that it works well in many materials.⁷⁴ However, it should be noted that the error

$$\Delta Q_8 - \Delta Q_7 = -\frac{\epsilon_1}{\delta_1} \Delta A = -\left(\frac{3\Delta_{\text{so}}}{3E_g + 2\Delta_{\text{so}}}\right) \Delta A \quad (36)$$

in making the replacement $\Delta Q_7 \rightarrow \Delta Q_8$ is of the same order as Δg in Eq. (25). In Sec. IV A it was argued

that Δg is not generally negligible. The error in ΔQ_7 is negligible in the present context not because ΔA is small (although it usually is), but because this error affects primarily only the spin-orbit split-off Γ_{7v} band. This band is typically not of direct experimental interest⁴⁸ unless $\Delta_{\text{so}} \ll E_g$, in which case the error (36) is negligible.

In a heterostructure, the linear changes are similar to the spin-zero expressions (30). In keeping with the PBA, only the Γ_8 results are given here:

$$\Delta Q^{\alpha\cdot} = -\frac{\epsilon_1 \Delta A^{\alpha\cdot}}{2E_g} - \frac{\epsilon_1 \Delta A}{2E_g} \left(\frac{E_{8v}^\alpha}{E_g} - \frac{\epsilon_1 E_v^\alpha}{\epsilon_2^2} \right), \quad (37a)$$

$$\Delta Q^{\cdot\alpha} = -\frac{2\epsilon_1 \Delta A^{\alpha\cdot}}{E_g} + \frac{\epsilon_1 \Delta A E_c^\alpha}{E_g} \left(\frac{1}{E_g} - \frac{\epsilon_1}{\epsilon_2^2} \right). \quad (37b)$$

The present method could, of course, be used without the PBA; this possibility is discussed below in Sec. IV D.

C. Choice of parameters

Procedures for choosing \bar{P} to avoid real spurious solutions have not yet been specified. In Sec. II B it was shown that spurious roots k_\perp^{sp} disappear at the zeros of the eigenvalues $\bar{d}_\nu(\hat{\mathbf{n}})$ of the matrix $\bar{D}(\hat{\mathbf{n}}) = \hat{n}_i \hat{n}_j \bar{D}^{ij}$. In the PB model, \bar{D} is block diagonal: $\bar{D} = \bar{D}^c \oplus \bar{D}^v$. The eigenvalues of the CB block $\bar{D}^c(\hat{\mathbf{n}})$ are independent of the direction $\hat{\mathbf{n}}$: $\bar{d}_\nu^c(\hat{\mathbf{n}}) = \bar{A}$ (where $\nu = 1, 2$). Thus, one can eliminate spurious solutions for all $\hat{\mathbf{n}}$ by setting $\bar{A} = 0$ or $\bar{P} = \bar{P}_c$, where

$$\bar{P}_c^2 = P^2 + \epsilon_1 A = \epsilon_1 / 2m_c. \quad (38)$$

This was the choice adopted in Ref. 32. As shown there, for typical semiconductors $|\epsilon_1 A| \ll P^2$, so $\bar{P}_c \approx P$ and the resulting changes in the Hamiltonian are small.³²

Other choices of \bar{P} can also be used to obtain physically meaningful results. In the limiting case $\bar{P} = 0$ of single-band effective-mass theory, all states within the energy gap are evanescent. Spurious solutions cannot be identified in this case because the CB and VB states are completely decoupled. For infinitesimal \bar{P} , there is an infinitesimal anticrossing of the evanescent gap states; the spurious solutions can then be identified as the branches with $\text{Im } k_\perp \neq 0$ over the entire range of energies near the band gap. Spurious gap modes remain evanescent for all $\hat{\mathbf{n}}$ in the finite interval $0 < \bar{P}^2 < \bar{P}_0^2$, where $\bar{P}_0^2 = \min(\bar{P}_c^2, \bar{P}_{v0}^2)$, $\bar{P}_{v0}^2 = \min_{\hat{\mathbf{n}}} \bar{P}_v^2(\hat{\mathbf{n}})$, and $\bar{P}_v^2(\hat{\mathbf{n}})$ is the smallest value of \bar{P}^2 where any $\bar{d}_\nu^v(\hat{\mathbf{n}}) = 0$.

As shown in Appendix C, when the Luttinger parameters satisfy $\gamma_3 \geq \gamma_2$ (which is true for most semiconductors^{58,60}), the constant \bar{P}_{v0}^2 is (in the PBA) simply

$$\bar{P}_{v0}^2 = P^2 - E_g L = -L^0 E_g. \quad (39)$$

If P^2 lies within the interval $0 < P^2 < \bar{P}_0^2$ —which is the case in the numerical examples considered below—then the spurious gap states in the original $\mathbf{k} \cdot \mathbf{p}$ Hamiltonian are evanescent for all $\hat{\mathbf{n}}$, and the Hamiltonian is physically

acceptable without any changes at all ($\Delta A = 0, \bar{P} = P$). If not, a valid alternative to setting $\bar{A} = 0$ is to choose a value of \bar{P}^2 within this interval,⁷ preferably near the upper bound \bar{P}_0^2 in order to minimize ΔP . For typical semiconductors both $|E_g L| \ll P^2$ and $|\epsilon_1 A| \ll P^2$, so the changes in the Hamiltonian are small regardless of whether \bar{P}_0^2 is equal to \bar{P}_c^2 or \bar{P}_{v0}^2 .

D. Beyond the Pidgeon–Brown approximation

The PBA used here is open to the objection that it does not provide an exact description of the mass of the spin-orbit split-off Γ_{7v} band⁴⁷ (although, as discussed above, it provides a good approximation in many cases⁷³). This deficiency can be remedied by applying the present unitary transformation to the Hamiltonian of Weiler *et al.*,⁷⁰ which includes a full set of independent parameters for Γ_{7v} . In particular, the momentum matrix element P has different values P_8 and P_7 for the coupling of Γ_{6c} to Γ_{8v} and Γ_{7v} , respectively. Equations (18) and (23) for the CB effective mass and g factor must therefore be replaced by

$$A + \frac{2P_8^2}{3E_g} + \frac{P_7^2}{3(E_g + \Delta_{\text{so}})} = \bar{A} + \frac{2\bar{P}_8^2}{3E_g} + \frac{\bar{P}_7^2}{3(E_g + \Delta_{\text{so}})} \quad (40)$$

and

$$g - \frac{4P_8^2}{3E_g} + \frac{4P_7^2}{3(E_g + \Delta_{\text{so}})} = \bar{g} - \frac{4\bar{P}_8^2}{3E_g} + \frac{4\bar{P}_7^2}{3(E_g + \Delta_{\text{so}})}. \quad (41)$$

Since there are two independent momentum parameters, one can choose the values of \bar{P}_8 and \bar{P}_7 in order to achieve desired changes in both A and g :

$$\bar{P}_8^2 = P_8^2 - E_g(\Delta A - \frac{1}{4}\Delta g), \quad (42a)$$

$$\bar{P}_7^2 = P_7^2 - (E_g + \Delta_{\text{so}})(\Delta A + \frac{1}{2}\Delta g). \quad (42b)$$

For example, one could choose $\Delta A = -A$ and $\Delta g = -g$ in order to set the entire CB \bar{D} matrix to zero. Alternatively, since g has no effect on spurious solutions, one could choose $\Delta g = 0$ in order to minimize the changes in the Hamiltonian. In either case, Eq. (9) can then be applied as usual to determine the changes in the other D parameters. However, since the Hamiltonian of Ref. 70 contains many parameters that are not commonly used in $\mathbf{k} \cdot \mathbf{p}$ calculations,⁶⁰ this procedure will not be carried out in detail here. In this case, it may be more convenient to calculate the Hamiltonian changes numerically using the matrix equations given in Appendix A.

E. Two-band model

In the special case of a bulk crystal with no spin-orbit coupling and $\mathbf{k} = (0, 0, k)$, the $|X\rangle$ and $|Y\rangle$ valence states are not coupled to the other states. Spurious solutions

in the PB model are consequently confined to the two-dimensional basis $\{|S\rangle, |Z\rangle\}$ with Hamiltonian

$$\bar{H}(k) = \begin{bmatrix} E_c + \bar{A}k^2 & i\bar{P}k \\ -i\bar{P}k & E_v + \bar{L}k^2 \end{bmatrix}. \quad (43)$$

This case is of interest^{14,15,20,27,46} because it allows simple analytical calculations of the properties of spurious solutions; it will also be used in some of the numerical work in Sec. V. The original Hamiltonian parameters are assumed to satisfy the constraints $E'_g = E_c - E_v > 0$ and

$$P^2 + E'_g A > 0, \quad P^2 - E'_g L > 0, \quad (44)$$

in which the first condition is equivalent to $m_c > 0$ [see Eq. (18)] and the second is equivalent to $L^0 < 0$ [see Eq. (28a)]. It is also assumed that $P^2 > 0$ and $\bar{P}^2 > 0$, which from Eq. (20) requires that $\Delta A < P^2/E'_g$.

The secular equation (12) for the Hamiltonian (43) has the form $c_4 k^4 + c_2 k^2 + c_0 = 0$, where $c_4 = \bar{A}\bar{L}$, $c_0 = (E_c - E)(E_v - E)$, and

$$c_2 = \bar{A}(E_v - E) + \bar{L}(E_c - E) - \bar{P}^2 \quad (45a)$$

$$= A(E_v - E) + L(E_c - E) - P^2, \quad (45b)$$

in which the second equality follows from Eqs. (18) and (28a). Hence, the coefficients c_0 and c_2 are invariant with respect to the unitary transformation (6). If the Hamiltonian (43) were extended to include terms of order k^4 , then c_4 would also be invariant,⁷⁵ but this would generate terms of higher order in the secular equation that are not invariant. In general, the highest-order coefficient in the (finite-order) secular equation is not invariant with respect to the unitary transformation (6).

The general solution to the secular equation is $k^2 = (-c_2 \pm \sqrt{c_2^2 - 4c_4 c_0})/2c_4$, which shows that for bounded c_1 , k is unbounded only when $c_4 \rightarrow 0$, as discussed in Secs. II B and IV C. The spurious solutions have a particularly simple form when $E = E_v$ or $E = E_c$:

$$k_{\text{sp}}^2(E_v) = (P^2 - E'_g L)/\bar{A}\bar{L}, \quad (46a)$$

$$k_{\text{sp}}^2(E_c) = (P^2 + E'_g A)/\bar{A}\bar{L}. \quad (46b)$$

For other values of E , note that $c_2(E)$ is a linear function of E that interpolates between the values $c_2(E_v) = -(P^2 - E'_g L)$ and $c_2(E_c) = -(P^2 + E'_g A)$. Thus, for small c_4 , $k_{\text{sp}}^2(E)$ interpolates approximately linearly between the values (46a) and (46b).

From Eq. (44), the numerators of Eqs. (46a) and (46b) are both positive. Therefore, the spurious solutions are evanescent when $\bar{A}\bar{L} < 0$ and propagating when $\bar{A}\bar{L} > 0$.^{20,27} Now $\bar{A}\bar{L} = AL + \Delta A(L - A) - (\Delta A)^2$ is a quadratic function of ΔA that has its maximum value when $\Delta A = \frac{1}{2}(L - A)$. According to Eq. (44), this value of ΔA satisfies the constraint $\Delta A < P^2/E'_g$ and is therefore permissible. When $\Delta A = \frac{1}{2}(L - A)$, $\bar{A} = \bar{L} = \frac{1}{2}(A + L)$ and thus

$$k_{\text{sp}}^2(E_v) = 4(P^2 - E'_g L)/(A + L)^2, \quad (47a)$$

$$k_{\text{sp}}^2(E_c) = 4(P^2 + E'_g A)/(A + L)^2. \quad (47b)$$

These expressions give the *smallest* positive values of $k_{\text{sp}}^2(E_{v,c})$ that are possible for any ΔA consistent with the given Hamiltonian parameters E'_g , P , A , and L . They consequently represent the “worst” result that could be obtained from any unitary transformation (6). For the special case $L = -A$, real spurious solutions do not exist for any ΔA , but for $L \neq -A$, real spurious solutions always exist for some ΔA .

It should be noted that the present theory provides the first rigorous justification for the two-band model of White and Sham,^{14,15} in which it is assumed to be possible always to choose $\bar{A} > 0$ and $\bar{L} < 0$ and to invoke the limit $\bar{A} \rightarrow 0$. The assumption $\bar{L} = -\bar{A}$, however, is not generally valid.

V. NUMERICAL EXAMPLES

Numerical examples demonstrating the success of the $\bar{A} = 0$ method in eliminating spurious solutions have already been given in Refs. 32 and 47. Since the present PB Hamiltonian for the case $\bar{A} = 0$ is identical to that of Ref. 32 in bulk material, those examples will not be repeated here. The main new feature is the interface operator ordering derived in Eqs. (21), (26), (30), and (37).

To demonstrate the validity of these results, the Γ_{15} valence⁷⁶ subband structure of $\text{In}_{0.53}\text{Ga}_{0.47}\text{As}/\text{InP}$ and GaAs/AlAs superlattices was calculated in a plane-wave basis using the ABINIT code^{77,78,79} with norm-conserving pseudopotentials and the local-density approximation (LDA). Spin-orbit coupling was omitted, and all technical details were the same as in Ref. 50. These “exact” model calculations were compared with the first-principles envelope-function (EF) theory of Refs. 49 and 51, which has no fitting parameters (not even the mean energy). As described in Sec. III, the EF Hamiltonian was constructed using nonlinear response theory; for this purpose, the bulk reference crystals were chosen to be $\text{In}_{0.765}\text{Ga}_{0.235}\text{As}_{0.5}\text{P}_{0.5}$ and $\text{Al}_{0.5}\text{Ga}_{0.5}\text{As}$.

A. Material parameters

Calculated values of the parameters in the Kane Hamiltonian are presented in Table I for the bulk materials of interest. This table includes values for the Kane parameter^{2,3} $B = D_{SZ}^{xy} + D_{SZ}^{yx}$, although this term is neglected in the PB model.⁴⁸ The values in Table I were calculated for the set $\mathcal{A} = \{\Gamma_{1c}, \Gamma_{15v}\}$, whereas those in Ref. 51 were for the single-band case $\mathcal{A} = \{\Gamma_{15v}\}$. The values of L , N , and K in Table I therefore differ from those in Table I of Ref. 51 because they do not include the interaction with the Γ_{1c} state $|S\rangle$. Since the coupling to the remote \mathcal{B} states is weaker in the present case, the parameters in Table I have a relatively small variation between materials, and the variation is nearly linear.

TABLE I: Material parameters for several bulk compounds and their virtual-crystal averages. The numbers in parentheses were obtained from linear interpolation. The signs of B and P depend on the phase conventions chosen for the basis functions. Here the coordinate origin was placed on an anion, with a neighboring cation at $\frac{1}{4}a(1, 1, 1)$; the phases were then fixed by setting $\langle \mathbf{x}|S \rangle > 0$ and $d\langle \mathbf{x}|X \rangle/dx > 0$ at $\mathbf{x} = \mathbf{0}$.

	GaAs	Al _{0.5} Ga _{0.5} As	AlAs
A	+0.280	+0.345	(+0.339)
B	-1.156	-0.837	(-0.777)
P	-0.560	-0.552	(-0.553)
L	-0.435	-0.345	(-0.343)
M	-1.511	-1.326	(-1.318)
N	-1.553	-1.373	(-1.366)
K	+2.507	+2.310	(+2.303)
	In _{0.53} Ga _{0.47} As	In _{0.765} Ga _{0.235} As _{0.5} P _{0.5}	InP
A	+0.321	+0.292	(+0.299)
B	-0.986	-0.954	(-0.927)
P	-0.534	-0.505	(-0.504)
L	-0.429	-0.413	(-0.410)
M	-1.385	-1.253	(-1.252)
N	-1.423	-1.296	(-1.292)
K	+2.370	+2.165	(+2.162)

To demonstrate the latter point, the numbers in parentheses in Table I give the parameters that would be obtained for the reference crystals if Vegard's law of linear interpolation were valid. Linear interpolation works well in all cases, with a maximum error of 7% in the B parameter for Al_{0.5}Ga_{0.5}As. This small error, in conjunction with the fact that the total variation is already a small perturbation, suggests that the linear perturbation theory developed in Sec. III should be a good approximation for the momentum and mass parameters. (Quadratic-response contributions are included in the present calculations,^{49,50,51} but only to order k^0 .)

Values for the linear heterostructure parameters defined in Secs. III and IV are listed in Table II. Here A^α denotes the total bulk value $A^\alpha \equiv A^{\alpha\alpha} + A^{\alpha\cdot} + A^{\alpha\cdot\cdot} = A^{\alpha\cdot} + 2A^{\alpha\cdot\cdot}$. The only other quantities not yet defined are the B parameters $B^{\alpha\cdot} = D_{SZ}^{x\alpha y} + D_{SZ}^{y\alpha x}$, $B^{\alpha\cdot\cdot} = D_{SZ}^{xy\alpha} + D_{SZ}^{yx\alpha}$, and $B^{\alpha\cdot\cdot\cdot} = D_{SZ}^{\alpha xy} + D_{SZ}^{\alpha yx}$. In this case $B^{\alpha\cdot\cdot\cdot} \neq B^{\alpha\cdot\cdot}$, so (unlike the other D terms) there are three independent linear parameters for B . The M and R values in Table II are the same as those in Table III of Ref. 51, but the other values are different.

The operator ordering given by the parameters in Table II does not seem to follow any simple general rules beyond the observation that $|P^{\alpha\cdot}| > |P^\alpha|$ for cation perturbations and $|P^{\alpha\cdot}| > |P^\alpha|$ for anion perturbations. In particular, the BenDaniel–Duke approximation,^{21,24,64} in which mass terms of the form $A^{\alpha\cdot}$, $B^{\alpha\cdot}$, etc., are assumed to be dominant, is clearly not valid in most cases. (See Ref. 51 for further discussion of this point.) However, since the linear changes are also small in most cases, the particular choice of operator ordering in the present multiband model is not as important as it would be in a

TABLE II: Linear parameters in the Γ_{1c} – Γ_{15v} Hamiltonian. Here RC stands for reference crystal, and the labels light and heavy holes refer to the bulk properties in the $\langle 100 \rangle$ directions.

RC		Al _{0.5} Ga _{0.5} As	In _{0.765} Ga _{0.235} As _{0.5} P _{0.5}
α		Ga	As
Conduction	A^α	-0.189	+0.090
	$A^{\alpha\cdot}$	+0.099	+0.039
	$A^{\alpha\cdot\cdot}$	-0.144	+0.026
Interband	B^α	-1.151	-0.023
	$B^{\alpha\cdot}$	+0.369	+0.104
	$B^{\alpha\cdot\cdot}$	-0.367	-0.162
	$B^{\alpha\cdot\cdot\cdot}$	-1.154	+0.035
Momentum	P^α	-0.019	-0.060
	$P^{\alpha\cdot}$	-0.027	-0.011
	$P^{\alpha\cdot\cdot}$	+0.008	-0.048
Light hole	L^α	-0.128	-0.037
	$L^{\alpha\cdot}$	+0.058	-0.081
	$L^{\alpha\cdot\cdot}$	-0.093	+0.022
Heavy hole	M^α	-0.387	-0.329
	$M^{\alpha\cdot}$	-0.039	-0.109
	$M^{\alpha\cdot\cdot}$	-0.174	-0.110
k^2 mixing	N^α	-0.319	-0.300
	$N^{\alpha\cdot}$	-0.136	-0.042
	$N^{\alpha\cdot\cdot}$	-0.091	-0.129
Landé	K^α	+0.464	+0.487
	$K^{\alpha\cdot}$	+0.034	+0.043
Rashba	$K^{\alpha\cdot\cdot}$	+0.215	+0.222
	R^α	-0.028	-0.017
δ mixing			

single-band model.

A comparison of the parameters in Tables I and II would seem to indicate some inconsistency in the calculation. For example, since the difference in Ga content between GaAs and AlAs is just 1, the linear bulk values A^α , B^α , etc., from Table II should be (approximately) numerically equal to the difference in the corresponding bulk constants of GaAs and AlAs from Table I (assuming that the variation is in fact linear, as suggested by the discussion of Table I above). However, $A(\text{GaAs}) - A(\text{AlAs}) = -0.119$, whereas $A^{\alpha=\text{Ga}} = -0.189$. The error of -0.069 in the value predicted by A^α is much larger than the error of -0.006 in the linear interpolation for A shown in Table I.

The reason for the discrepancy is the different methods used to eliminate interband coupling in the two cases. The bulk parameters in Table I were calculated by first diagonalizing the entire $(\mathcal{A} + \mathcal{B})$ Hamiltonian at $\mathbf{k} = \mathbf{0}$ exactly, and then using perturbation theory to eliminate the $\mathbf{k} \cdot \mathbf{p}$ coupling between \mathcal{A} and \mathcal{B} . However, in the linear-response theory of Refs. 49 and 51, the \mathbf{k} -independent heterostructure perturbation and the $\mathbf{k} \cdot \mathbf{p}$ terms are all block-diagonalized together using a single unitary transformation.^{80,81} Since the heterostructure perturbation X and the $\mathbf{k} \cdot \mathbf{p}$ perturbation Y do not commute, we have $e^{S(X+Y)} \neq e^{S(X)}e^{S(Y)}$, and the two unitary transformations yield different bulk Hamiltonian matrices for set \mathcal{A} . But the difference is merely a \mathbf{k} -dependent unitary transformation of the form defined

TABLE III: Error in linear-response prediction of the difference in effective-mass parameters for bulk materials A and B. These values should satisfy Eq. (29) if the “error” is not really an error but arises only from a unitary transformation.

A/B	GaAs/AlAs	In _{0.53} Ga _{0.47} As/InP
ΔA	-0.069	-0.036
ΔL	+0.056	+0.043
ΔM	-0.001	-0.002
ΔN	+0.056	+0.041
ΔK	+0.057	+0.045

previously in Eqs. (6) and (7).

To demonstrate this, the “errors” in the predictions obtained from Table II for the differences in A , L , M , N , and K between materials A and B (e.g., GaAs and AlAs) were calculated from expressions of the form

$$\Delta L = \sum_{\alpha} [\theta_{\alpha}(A) - \theta_{\alpha}(B)] L^{\alpha} - [L(A) - L(B)]. \quad (48)$$

The results are shown in Table III. If the discrepancy is really due to a unitary transformation of the form (6), these errors should obey the relations given previously in Eq. (29). These relations are clearly not satisfied exactly, but the deviation from a pure unitary transformation, if divided equally between conduction and valence bands, amounts to only about 0.007 for GaAs/AlAs and 0.004 for In_{0.53}Ga_{0.47}As/InP. This is just the magnitude of the linear interpolation error for these parameters shown in Table I.

Hence, a careful examination of the material parameters shows that a linear approximation should work very well for the effective-mass and momentum terms. However, it should be noted that the perturbation theory of Refs. 49 and 51 yields a $\mathbf{k} \cdot \mathbf{p}$ Hamiltonian that already includes a unitary transformation of the form (6) relative to the conventional Kane form of the $\mathbf{k} \cdot \mathbf{p}$ Hamiltonian. (As discussed in Sec. IID, this is also the case for most empirical $\mathbf{k} \cdot \mathbf{p}$ data sets found in the literature; the difference here is that in the present theory the effect of this transformation is *known* and has already been accounted for in the operator ordering for heterostructures.)

B. Valence subband structure

As a direct test of the present theory, the Γ_{15} valence⁷⁶ subband structure was calculated numerically for In_{0.53}Ga_{0.47}As/InP and GaAs/AlAs superlattices in the LDA model system described above.^{50,51} The transformation (6) was applied to the set $\mathcal{A} = \{\Gamma_{1c}, \Gamma_{15v}\}$ with $\bar{A} = \lambda A$ for the reference crystal and $\bar{A}^{\alpha\alpha} = \delta_{\lambda,1} A^{\alpha\alpha}$, $\bar{A}^{\alpha\alpha} = \delta_{\lambda,1} A^{\alpha\alpha}$ for the linear response, where λ is a real parameter. Choosing $\lambda = 1$ gives no transformation at all, but any value $\lambda \neq 1$ modifies the bulk value of A and (for simplicity) sets the linear position dependence of \bar{A} to zero.

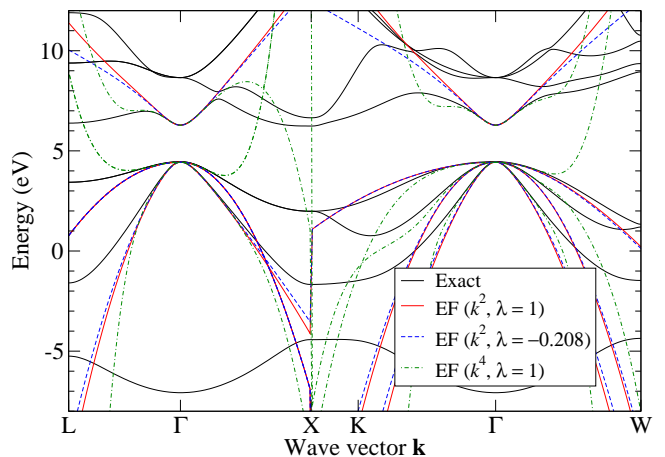


FIG. 1: (Color online) Energy band structure of the bulk In_{0.765}Ga_{0.235}As_{0.5}P_{0.5} reference crystal: comparison of exact calculation with 4-state $\mathbf{k} \cdot \mathbf{p}$ models.

To determine the effect of different choices of λ , recall from Sec. IVE that the spurious solutions for $\mathbf{k} \parallel \langle 100 \rangle$ are evanescent when $\bar{A}\bar{L} < 0$ and propagating when $\bar{A}\bar{L} > 0$. From Eq. (29) we have $\Delta L = -\Delta A$, hence $\bar{L} = L - (\lambda - 1)A$. Thus, \bar{A} changes sign at $\lambda = 0$, whereas \bar{L} changes sign at $\lambda = 1 + L/A$. Putting in the values of A and L for the reference crystals in Table II, one finds that for $\lambda = 1$, the spurious solutions for In_{0.765}Ga_{0.235}As_{0.5}P_{0.5} are evanescent, but values of λ in the range $-0.415 < \lambda < 0$ yield spurious propagating modes. However, for Al_{0.5}Ga_{0.5}As, where $L \approx -A$, spurious propagating modes occur only in the narrow region $0 < \lambda < 0.002$.

To obtain the most rigorous test of the present theory, one can seek out the “worst case” value of λ that gives real spurious wave vectors with the smallest magnitude. As shown in Sec. IVE, this case corresponds to $\bar{A} = \bar{L} = \frac{1}{2}(A + L)$ or $\lambda = \lambda_0 = \frac{1}{2}(1 + L/A)$, which is halfway between the sign changes for \bar{A} and \bar{L} . Since $L \approx -A$ for Al_{0.5}Ga_{0.5}As, Eq. (47) shows that even the “worst case” real spurious solutions in this material will have extremely large wave vectors. Therefore, in what follows, only the In_{0.53}Ga_{0.47}As/InP material system is studied in detail, as this provides a more stringent test. In this system, the In_{0.765}Ga_{0.235}As_{0.5}P_{0.5} reference crystal has $\lambda_0 = -0.208$.

The energy band structure for In_{0.765}Ga_{0.235}As_{0.5}P_{0.5} is shown in Fig. 1, which compares the “exact” solutions of the model Hamiltonian with various $\mathbf{k} \cdot \mathbf{p}$ models. The $\mathbf{k} \cdot \mathbf{p}$ calculations for $\lambda = 1$ and $\lambda = -0.208$ are very similar for small k , but are visibly different for \mathbf{k} near the Brillouin zone boundary. The real spurious solutions for $\lambda = -0.208$ and $\mathbf{k} \parallel \langle 100 \rangle$ occur at $k \simeq \pm 15(2\pi/a)$, where a is the cubic lattice constant. Also shown in Fig. 1 are the results when the $\mathbf{k} \cdot \mathbf{p}$ Hamiltonian is extended^{49,51} to include terms of order k^3 and k^4 ; this case has more obvious spurious solutions that occur well inside the Brillouin zone.

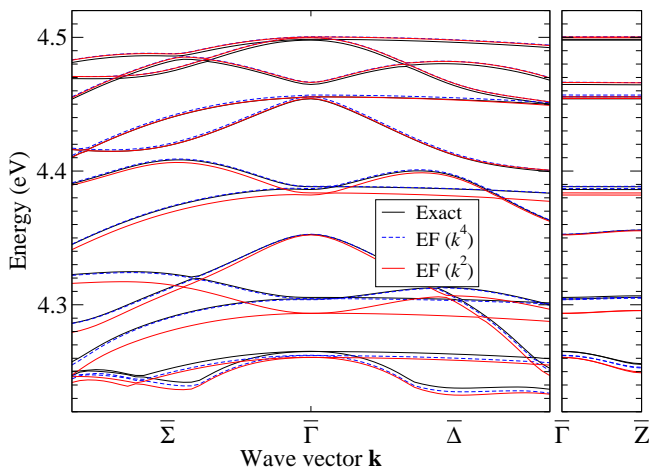


FIG. 2: (Color online) Γ_{15} valence subband structure of a (001) $(\text{In}_{0.53}\text{Ga}_{0.47}\text{As})_{24}(\text{InP})_{24}$ superlattice.

The valence subband structure of a (001) $(\text{In}_{0.53}\text{Ga}_{0.47}\text{As})_{24}(\text{InP})_{24}$ superlattice was calculated for a series of $O(k^2)$ EF models with $\lambda = 1, 0.5, 0, -0.208, -0.5,$ and -1 . These calculations were performed in momentum space⁶⁹ with a basis containing 25 EF plane waves (corresponding to a plane-wave cutoff at half the distance to the bulk X point). Since the real spurious solutions occur at $|k| \gtrsim 15(2\pi/a)$, such a cutoff is sufficient to filter out the spurious modes^{25,32,47} for any value of λ .

The results of these calculations are shown in Fig. 2. The entire range $-1 \leq \lambda \leq 1$ is designated by the single label $\text{EF}(k^2)$, since these values cannot be distinguished at this scale—they differ by no more than 0.1 meV for the top five subbands and by no more than 0.3 meV for any of the 12 subbands shown. The agreement with the exact calculations is excellent for the top five subbands (with a mean error in each subband of less than 1.8 meV), but it begins to deteriorate for energies more than 100 meV below the band edge. This discrepancy is due primarily to the neglect of terms of order k^4 in the bulk reference Hamiltonian. When these are included⁵¹ [see curves labeled $\text{EF}(k^4)$], the agreement is much improved, with a maximum mean error of 3 meV for the top 12 subbands. For the $O(k^4)$ calculations, the number of plane waves was reduced to 17 (i.e., one-third of the Brillouin zone) in order to avoid problems from the real spurious solutions in Fig. 1.

The good agreement shown in Fig. 2 confirms the validity of both the operator ordering derived here and the linear-response approximation used for π^i and D^{ij} in the multiband EF Hamiltonian. (Quadratic-response terms were included only in the potential energy.^{49,50,51}) Note that the 0.3 meV variation for $-1 \leq \lambda \leq 1$ is an order of magnitude smaller than the 5 meV variation shown in Fig. 2 of Ref. 32, which did not account for changes in operator ordering.

VI. DISCUSSION AND CONCLUSIONS

In conclusion, the unitary transformation (6) eliminates spurious solutions in the Kane model with no approximation beyond the limitation to second-order differential operators. A comparison of the derived operator ordering with density-functional calculations of the valence subband structure shows very good agreement.

This good agreement was obtained using a linear-response approximation for the material dependence of the partially renormalized multiband effective-mass and momentum parameters, with quadratic “bowing” terms included only for the band-edge energies. As shown in Sec. V A, such an approximation is justified in a multiband Hamiltonian because (unlike the single-band case⁵¹) the corrections due to renormalization from the remote \mathcal{B} states have a relatively weak variation between materials. Indeed, the present description of material properties is almost identical to the interpolation scheme for the conduction-band mass of ternary alloys recommended on page 5837 of Vurgaftman *et al.*⁶⁰ (although it should be noted that this scheme was not used uniformly for all effective-mass parameters in Ref. 60). The only difference is that the present work treats P as linear, whereas Vurgaftman *et al.* treat P^2 as linear.⁶⁰

It should be noted that the linear Hamiltonian (14) is expressed in an atomistic form, as the superposition of responses to individual atomic perturbations. This is the simplest and most natural way of expressing the results of linear response theory. Such a description may be unfamiliar to many readers since most envelope-function models are formulated in terms of bulk compounds rather than atoms. However, as shown in Sec. VII A of Ref. 49, a traditional bulk-crystal description can be obtained from the present atomistic formulation via a straightforward linear transformation of variables (bearing in mind that the “bulk” compounds for the no-common-atom $\text{In}_{0.53}\text{Ga}_{0.47}\text{As}/\text{InP}$ material system must include not just $\text{In}_{0.53}\text{Ga}_{0.47}\text{As}$ and InP but also the interface materials InAs and $\text{In}_{0.53}\text{Ga}_{0.47}\text{P}$). Nevertheless, there are advantages to becoming familiar with both points of view, since the atomistic perspective is simpler and better suited for the description of complex nanostructures.

Most envelope-function models are also expressed in a general form that allows the inclusion of arbitrary nonlinear material dependence in the effective-mass and momentum terms. However, the ability to include nonlinear terms does not necessarily imply greater accuracy, since the present results show that the operator ordering used in most envelope-function models is not correct even to linear order. The possibility of applying the present unitary transformation to a more general phenomenological Hamiltonian with arbitrary nonlinear material dependence was examined during the development of this paper, but since the interface structure of the resulting theory is much more complicated than the linear theory, it was not considered worthwhile to publish the nonlinear results. The linear approach has the advantage of pro-

viding simple analytical expressions for precisely those terms that are of greatest importance in a multiband envelope-function theory.

For practical problems, a full implementation of the operator ordering derived here would require the knowledge of many parameters that have not been measured experimentally and cannot yet be predicted accurately from first principles. Therefore, in the near future, any practical application of the theory based purely on existing empirical data will require the use of some approximations. This point is underscored by the results obtained in Sec. IID, which show that the bulk $\mathbf{k} \cdot \mathbf{p}$ parameters generated by typical experimental data-fitting procedures already include a unitary transformation—of unknown magnitude—of the type defined here. The uncertainty would seem to be greatest for the convenient tabulations in review articles⁶⁰ of parameters compiled from many sources.

Given such uncertainty in the existing experimental data, it is reasonable to base short-term applications of the present theory on the criterion of simplicity rather than theoretical rigor. If an unknown bulk unitary transformation is already present in the empirical parameters, the original LK basis cannot be defined experimentally, and it is not possible to make any definite statements about operator ordering in heterostructures. Therefore, one might as well choose something simple, such as the conventional BenDaniel–Duke operator ordering. For simplicity, one can apply this operator ordering *after* a bulk unitary transformation has been used to eliminate real spurious solutions, as in the heuristic model of Ref. 32.

Two choices of unitary transformations in heterostructures stand out for their simplicity. One is to set $\bar{A} = 0$ everywhere,³² which has computational advantages¹² because it allows the conduction-band envelopes to be eliminated from explicit appearance in the envelope-function equations.³² The other is to select a single value of \bar{P} for the entire heterostructure,^{18,27} which is chosen to yield evanescent spurious solutions in accordance with the guidelines given in Sec. IV C. Assuming that $\bar{A} \neq 0$, this choice simplifies the interface boundary conditions (for calculations based on the flat-band approximation) because it ensures continuity of all envelopes.^{14,15}

The above approach is merely a quick practical fix in which the uncertainty in experimental parameters is openly acknowledged and even turned to advantage by selecting simple operator ordering and a parameter set with no real spurious solutions. The resulting errors in operator ordering—which are probably systematic—are simply ignored.

However, it is hoped that the present theory will also provide a stimulus for future work in which the sources of ambiguity in our present knowledge are steadily eliminated. With a careful combination of experimental data and empirically-based microscopic theory (such as empirical pseudopotentials⁶² or empirical tight-binding theory⁶³) it should be possible to establish for each mate-

rial whether spurious solutions in the Kane Hamiltonian are really required by experiment or are merely an artifact of current data-fitting procedures. Application of the same methods to heterostructures will provide more definitive results for the parameters that determine operator ordering. At the same time, extensions of the present *ab initio* techniques to include quasiparticle self-energies and projector-augmented waves should provide more accurate predictions of parameters from first principles. It is hoped that at some time in the near future these two lines of investigation will converge to yield a practical $\mathbf{k} \cdot \mathbf{p}$ theory free from ambiguity.

Acknowledgments

This work was supported by Hong Kong RGC Grant No. 600905.

APPENDIX A: MATRIX FORMULATION OF HAMILTONIAN CHANGES

Let $H_m^{(n)}$ be the contribution to the matrix H that is of order $\theta^n k^m$, where θ is the heterostructure perturbation parameter introduced in Eq. (14a). Then the changes in the reference crystal Hamiltonian (1) due to the unitary transformation (6) are given by [cf. Eq. (9)]

$$\Delta H_1^{(0)} = [H_0^{(0)}, S_1^{(0)}], \quad (\text{A1})$$

$$\Delta H_2^{(0)} = [\tilde{H}_1^{(0)}, S_1^{(0)}] + [H_0^{(0)}, S_2^{(0)}], \quad (\text{A2})$$

while the changes in the linear Hamiltonian (14) are [cf. Eqs. (16) and (17)]

$$\Delta H_1^{(1)} = [H_0^{(1)}, S_1^{(0)}] + [H_0^{(0)}, S_1^{(1)}], \quad (\text{A3})$$

$$\begin{aligned} \Delta H_2^{(1)} = & [\tilde{H}_1^{(1)}, S_1^{(0)}] + [\tilde{H}_1^{(0)}, S_1^{(1)}] \\ & + [H_0^{(1)}, S_2^{(0)}] + [H_0^{(0)}, S_2^{(1)}], \end{aligned} \quad (\text{A4})$$

in which $\tilde{H}_1^{(n)} = H_1^{(n)} + \frac{1}{2}\Delta H_1^{(n)}$.

APPENDIX B: COORDINATE AND VELOCITY

This appendix examines the effect of the transformation (6) on the coordinate and velocity. In the LK representation, the coordinate operator inside the first Brillouin zone is just $i\nabla_{\mathbf{k}}\delta_{nn'}$.⁵² After the $\mathbf{k} \cdot \mathbf{p}$ coupling between \mathcal{A} and \mathcal{B} is eliminated, the effective coordinate for \mathcal{A} becomes

$$\langle n\mathbf{k} | \mathbf{x} | n'\mathbf{k}' \rangle = \mathbf{x}_{nn'}(\mathbf{k})\delta(\mathbf{k} - \mathbf{k}'), \quad (\text{B1a})$$

in which the operator $\mathbf{x}_{nn'}(\mathbf{k})$ is given to first order in k by

$$\mathbf{x}_{nn'}(\mathbf{k}) = i\nabla_{\mathbf{k}}\delta_{nn'} + \frac{1}{2}\boldsymbol{\Omega}_{nn'} \times \mathbf{k}. \quad (\text{B1b})$$

Here $\mathbf{\Omega}_{nn'}$ is the Berry curvature^{82,83,84,85,86} at $\mathbf{k} = \mathbf{0}$ for the quasi-Bloch (or transformed LK) basis:

$$\mathbf{\Omega}_{nn'} = i \sum_l^B \boldsymbol{\xi}_{nl} \times \boldsymbol{\xi}_{ln'}, \quad (\text{B2})$$

in which $\boldsymbol{\xi}_{nn'}$ is the crystal coordinate⁸⁷ or Berry connection⁸⁵

$$\boldsymbol{\xi}_{nn'} = \frac{-i\boldsymbol{\pi}_{nn'}}{\omega_{nn'}} \quad (E_n \neq E_{n'}). \quad (\text{B3})$$

The effective velocity $\mathbf{v} = -i[\mathbf{x}, H]$ for \mathcal{A} is therefore given (to first order in k) by

$$\mathbf{v}_{nn'}(\mathbf{k}) = \nabla_{\mathbf{k}} H_{nn'}(\mathbf{k}) + \frac{i\omega_{nn'}}{2} \mathbf{\Omega}_{nn'} \times \mathbf{k}. \quad (\text{B4})$$

Here the contribution from $\mathbf{\Omega}_{nn'}$ vanishes in a single-band effective-mass model, but not in a multiband model. This contribution is related⁸⁸ to the so-called anomalous velocity^{82,83} or Hall velocity⁸⁶ in an external field. $\mathbf{\Omega}$ is a hermitian operator with the same symmetry as an angular momentum or a magnetic field (i.e., $\mathbf{\Omega}$ is a pseudovector that is odd under time reversal). In a zincblende crystal, $\mathbf{\Omega}$ has $\Gamma_{25'}$ symmetry and couples the Γ_6 conduction band to the Γ_8 valence band in the presence of spin-orbit coupling.

After the transformation $\bar{\mathbf{x}} = e^{-S} \mathbf{x} e^S$, the effective coordinate for \mathcal{A} becomes

$$\begin{aligned} \bar{\mathbf{x}}_{nn'}(\mathbf{k}) = & i \nabla_{\mathbf{k}} \delta_{nn'} + \Delta \boldsymbol{\xi}_{nn'} + \frac{1}{2} \bar{\mathbf{\Omega}}_{nn'} \times \mathbf{k} \\ & + i \hat{\mathbf{x}}_j (S_{nn'}^{jl} + S_{nn'}^{lj}) k_l, \end{aligned} \quad (\text{B5})$$

in which $\Delta \boldsymbol{\xi}_{nn'} = +i \Delta \boldsymbol{\pi}_{nn'} / \omega_{nn'}$ and $\bar{\mathbf{\Omega}}_{nn'} = \mathbf{\Omega}_{nn'} + \Delta \mathbf{\Omega}_{nn'}$, where

$$\Delta \mathbf{\Omega}_{nn'} = i \sum_l^A \Delta \boldsymbol{\xi}_{nl} \times \Delta \boldsymbol{\xi}_{ln'}. \quad (\text{B6})$$

The transformed velocity $\bar{\mathbf{v}} = e^{-S} \mathbf{v} e^S = -i[\bar{\mathbf{x}}, \bar{H}]$ is given by Eq. (13). In this case, attempting to write $\bar{\mathbf{v}}$

in a form analogous to Eq. (B4) yields a rather lengthy expression that is not given here.

APPENDIX C: EQUATION (39)

This appendix contains a derivation of the expression for $\bar{P}_{\nu 0}^2 = \min_{\hat{\mathbf{n}}} \bar{P}_{\nu}^2(\hat{\mathbf{n}})$ given in Eq. (39) of Sec. IV C. Here $\bar{P}_{\nu}^2(\hat{\mathbf{n}})$ is the smallest value of \bar{P}^2 where any eigenvalue $\bar{d}_{\nu}^2(\hat{\mathbf{n}}) = 0$. To find the value of $\bar{P}_{\nu 0}^2$ it is therefore necessary to determine the direction $\hat{\mathbf{n}}$ in which $\bar{d}_{\nu}^2(\hat{\mathbf{n}})$ first reaches zero (for any ν or $\hat{\mathbf{n}}$) as \bar{P}^2 is increased from zero.

The problem can be simplified by noting that in the PBA, the 6×6 VB block $\bar{D}^{\nu}(\hat{\mathbf{n}})$ can be further reduced to the direct sum of two 3×3 spin-zero blocks, since the mass parameters in the PBA do not depend on spin. The eigenvalues of these 3×3 matrices cannot be found analytically for general $\hat{\mathbf{n}}$, but a useful approximate solution can be obtained from a rotated basis¹ $\{|X'\rangle, |Y'\rangle, |Z'\rangle\}$ in which $|Z'\rangle = \hat{n}_x |X\rangle + \hat{n}_y |Y\rangle + \hat{n}_z |Z\rangle$. In this basis, the $|Z'\rangle$ state is of principal interest because $|X'\rangle$ and $|Y'\rangle$ are not coupled to the CB by the $\mathbf{k} \cdot \mathbf{p}$ interaction. The corresponding diagonal matrix element of $D^{\nu}(\hat{\mathbf{n}})$ is

$$D_{Z'Z'}^{\nu}(\hat{\mathbf{n}}) = L - 2(L - M - N)(\hat{n}_y^2 \hat{n}_z^2 + \hat{n}_z^2 \hat{n}_x^2 + \hat{n}_x^2 \hat{n}_y^2). \quad (\text{C1})$$

For $\hat{\mathbf{n}}$ in the $\langle 100 \rangle$, $\langle 110 \rangle$, and $\langle 111 \rangle$ directions, the matrix $D^{\nu}(\hat{\mathbf{n}})$ is diagonal and Eq. (C1) is an exact eigenvalue. For other directions, Eq. (C1) is not an exact eigenvalue, but it does provide a useful qualitative description of the angular dependence of the exact solution.

In typical semiconductors, the Luttinger parameters (original⁶⁶ or modified⁴⁸) satisfy $\gamma_3 > \gamma_2$,^{58,60} hence $L - M - N = 3(\gamma_3 - \gamma_2) > 0$. Equation (C1) therefore suggests that the first eigenvalue $\bar{d}_{\nu}^2(\hat{\mathbf{n}})$ (for any direction $\hat{\mathbf{n}}$) to reach $\bar{d}_{\nu}^2(\hat{\mathbf{n}}) = 0$ as \bar{P} increases from zero will be the eigenvalue \bar{L} corresponding to a state $|Z'\rangle$ with $\hat{\mathbf{n}} \parallel \langle 100 \rangle$. This tentative conclusion has been confirmed by a numerical examination of the eigenvalues $\bar{d}_{\nu}^2(\hat{\mathbf{n}})$ in different directions as \bar{P} is varied.

Therefore, when $\gamma_3 \geq \gamma_2$ (as is usually the case), the constant $\bar{P}_{\nu 0}^2$ is given by Eq. (39).

* Electronic address: phbaf@ust.hk

¹ E. O. Kane, J. Phys. Chem. Solids **1**, 249 (1957).

² E. O. Kane, in *Semiconductors and Semimetals*, edited by R. K. Willardson and A. C. Beer (Academic, New York, 1966), vol. 1, pp. 75–100.

³ E. O. Kane, in *Narrow Gap Semiconductors: Physics and Applications*, edited by W. Zawadzki (Springer, Berlin, 1980), vol. 133 of *Lecture Notes in Physics*, pp. 13–31.

⁴ G. A. Sai-Halasz, R. Tsu, and L. Esaki, Appl. Phys. Lett. **30**, 651 (1977).

⁵ V. Mlinar, M. Tadić, B. Partoens, and F. M. Peeters, Phys. Rev. B **71**, 205305 (2005).

⁶ E. G. Novik, A. Pfeuffer-Jeschke, T. Jungwirth, V. Latussek, C. R. Becker, G. Landwehr, H. Buhmann, and L. W. Molenkamp, Phys. Rev. B **72**, 035321 (2005).

⁷ S. v Alftan, F. Boxberg, K. Kaski, A. Kuronen, R. Tereshonkov, J. Tulkki, and H. Sakaki, Phys. Rev. B **72**, 045329 (2005).

⁸ T. Koprucki, M. Baro, U. Bandelow, T. Q. Tien, F. Weik, J. W. Tomm, M. Grau, and M.-C. Amann, Appl. Phys. Lett. **87**, 181911 (2005).

⁹ A. V. Maslov and C. Z. Ning, Phys. Rev. B **72**, 161310(R) (2005).

¹⁰ K. Nilsson, A. Zakharova, I. Lapushkin, S. T. Yen, and

- K. A. Chao, Phys. Rev. B **74**, 075308 (2006).
- ¹¹ F. Boxberg, R. Tereshonkov, and J. Tulkki, J. Appl. Phys. **100**, 063108 (2006).
- ¹² H.-B. Wu, S. J. Xu, and J. Wang, Phys. Rev. B **74**, 205329 (2006).
- ¹³ B. Lassen, M. Willatzen, R. Melnik, and L. C. Lew Yan Voon, J. Mater. Res. **21**, 2927 (2006).
- ¹⁴ S. R. White and L. J. Sham, Phys. Rev. Lett. **47**, 879 (1981).
- ¹⁵ S. R. White, G. E. Marques, and L. J. Sham, J. Vac. Sci. Technol. **21**, 544 (1982).
- ¹⁶ M. F. H. Schuurmans and G. W. 't Hooft, Phys. Rev. B **31**, 8041 (1985).
- ¹⁷ D. L. Smith and C. Mailhot, Phys. Rev. B **33**, 8345 (1986).
- ¹⁸ R. Eppenga, M. F. H. Schuurmans, and S. Colak, Phys. Rev. B **36**, 1554 (1987).
- ¹⁹ L. R. Ram-Mohan, K. H. Yoo, and R. L. Aggarwal, Phys. Rev. B **38**, 6151 (1988).
- ²⁰ W. Trzeciakowski, Phys. Rev. B **38**, 12493 (1988).
- ²¹ G. Bastard, *Wave Mechanics Applied to Semiconductor Heterostructures* (Wiley, New York, 1988).
- ²² D. L. Smith and C. Mailhot, Rev. Mod. Phys. **62**, 173 (1990).
- ²³ C. Mailhot and D. L. Smith, J. Vac. Sci. Technol. B **8**, 793 (1990).
- ²⁴ G. Bastard, J. A. Brum, and R. Ferreira, in *Solid State Physics*, edited by H. Ehrenreich and D. Turnbull (Academic, Boston, 1991), vol. 44, pp. 229–415.
- ²⁵ R. Winkler and U. Rössler, Phys. Rev. B **48**, 8918 (1993).
- ²⁶ C. Aversa and J. E. Sipe, Phys. Rev. B **49**, 14542 (1994).
- ²⁷ A. T. Meney, B. Gonul, and E. P. O'Reilly, Phys. Rev. B **50**, 10893 (1994).
- ²⁸ K. J. Duff, Aust. J. Phys. **47**, 77 (1994).
- ²⁹ F. Szmulowicz and G. J. Brown, Phys. Rev. B **51**, 13203 (1995).
- ³⁰ M. J. Godfrey and A. M. Malik, Phys. Rev. B **53**, 16504 (1996).
- ³¹ F. Szmulowicz, Phys. Rev. B **54**, 11539 (1996).
- ³² B. A. Foreman, Phys. Rev. B **56**, R12748 (1997).
- ³³ For readers of Ref. 32 who wonder what “envelope structure theory” is, this phrase was coined by an overzealous editor—after final proof corrections—as an abridgment of “heterostructure envelope-function theory.”
- ³⁴ M. G. Burt, Superlattices Microstruct. **23**, 531 (1998).
- ³⁵ M. V. Kisin, B. L. Gelmont, and S. Luryi, Phys. Rev. B **58**, 4605 (1998).
- ³⁶ Al. L. Efros and M. Rosen, Phys. Rev. B **58**, 7120 (1998).
- ³⁷ M. G. Burt, J. Phys.: Condens. Matter **11**, R53 (1999).
- ³⁸ P. C. Sercel, Al. L. Efros, and M. Rosen, Phys. Rev. Lett. **83**, 2394 (1999).
- ³⁹ L.-W. Wang, Phys. Rev. B **61**, 7241 (2000).
- ⁴⁰ W. Jaskólski, R. Oszwaldowski, and G. W. Bryant, Vacuum **63**, 191 (2001).
- ⁴¹ A. V. Rodina, A. Yu. Alekseev, Al. L. Efros, M. Rosen, and B. K. Meyer, Phys. Rev. B **65**, 125302 (2002).
- ⁴² M. Holm, M.-E. Pistol, and C. Pryor, J. Appl. Phys. **92**, 932 (2002).
- ⁴³ X. Cartoixà, D. Z.-Y. Ting, and T. C. McGill, J. Appl. Phys. **93**, 3974 (2003).
- ⁴⁴ K. I. Kolokolov, J. Li, and C. Z. Ning, Phys. Rev. B **68**, 161308(R) (2003).
- ⁴⁵ F. Szmulowicz, Europhys. Lett. **69**, 249 (2005).
- ⁴⁶ F. Szmulowicz, Phys. Rev. B **71**, 245117 (2005).
- ⁴⁷ W. Yang and K. Chang, Phys. Rev. B **72**, 233309 (2005).
- ⁴⁸ C. R. Pidgeon and R. N. Brown, Phys. Rev. **146**, 575 (1966).
- ⁴⁹ B. A. Foreman, Phys. Rev. B **72**, 165345 (2005).
- ⁵⁰ B. A. Foreman (2007), cond-mat/0703697.
- ⁵¹ B. A. Foreman (2007), cond-mat/0701396.
- ⁵² J. M. Luttinger and W. Kohn, Phys. Rev. **97**, 869 (1955).
- ⁵³ G. L. Bir and G. E. Pikus, *Symmetry and Strain-Induced Effects in Semiconductors* (Wiley, New York, 1974).
- ⁵⁴ C. Cohen-Tannoudji, J. Dupont-Roc, and G. Grynberg, *Photons and Atoms: Introduction to Quantum Electrodynamics* (Wiley, New York, 1989).
- ⁵⁵ J. J. Sakurai, *Advanced Quantum Mechanics* (Addison-Wesley, Reading, MA, 1967), p. 78.
- ⁵⁶ It is possible that the real spurious solutions produced by $O(k^4)$ terms in the multiband Hamiltonian could be eliminated by extending the generator S in Eq. (7) to include terms of order k^3 , but this possibility will not be considered further here.
- ⁵⁷ L. M. Roth, B. Lax, and S. Zwerdling, Phys. Rev. **114**, 90 (1959).
- ⁵⁸ P. Lawaetz, Phys. Rev. B **4**, 3460 (1971).
- ⁵⁹ C. Hermann and C. Weisbuch, in *Optical Orientation*, edited by F. Meier and B. P. Zakharchenya (North-Holland, Amsterdam, 1984), chap. 11, pp. 463–508.
- ⁶⁰ I. Vurgaftman, J. R. Meyer, and L. R. Ram-Mohan, J. Appl. Phys. **89**, 5815 (2001).
- ⁶¹ R. L. Aggarwal, Phys. Rev. B **2**, 446 (1970).
- ⁶² H. Fu and A. Zunger, Phys. Rev. B **55**, 1642 (1997).
- ⁶³ J.-M. Jancu, R. Scholz, E. A. de Andrada e Silva, and G. C. La Rocca, Phys. Rev. B **72**, 193201 (2005).
- ⁶⁴ D. J. BenDaniel and C. B. Duke, Phys. Rev. **152**, 683 (1966).
- ⁶⁵ For examples illustrating the transformation of operators from momentum to coordinate space, see Eqs. (22.10b) and (22.14c) of Bir and Pikus⁵³ and Eqs. (3b) and (4) of Winkler and Rössler.²⁵
- ⁶⁶ J. M. Luttinger, Phys. Rev. **102**, 1030 (1956).
- ⁶⁷ The term P^α (but not $P^{\alpha'}$) was also excluded in Ref. 32 because of a mathematical conflict in the model with $\bar{A} = 0$ and piecewise-constant material parameters. This conflict remains, but the correct resolution is not to abandon the operator ordering derived from first principles. Rather, one should reject discontinuous parameters as physically unrealistic.
- ⁶⁸ J. C. Hensel and K. Suzuki, Phys. Rev. Lett. **22**, 838 (1969).
- ⁶⁹ D. Gershoni, C. H. Henry, and G. A. Baraff, IEEE J. Quantum Electron. **29**, 2433 (1993).
- ⁷⁰ M. H. Weiler, R. L. Aggarwal, and B. Lax, Phys. Rev. B **17**, 3269 (1978).
- ⁷¹ H.-R. Trebin, U. Rössler, and R. Ranvaud, Phys. Rev. B **20**, 686 (1979).
- ⁷² H.-R. Trebin, B. Wolfstädter, H. Pascher, and H. Häfele, Phys. Rev. B **37**, 10249 (1988).
- ⁷³ K. Boujdaria, S. Ridene, and G. Fishman, Phys. Rev. B **63**, 235302 (2001).
- ⁷⁴ Boujdaria *et al.*⁷³ did not study explicitly the error generated by treating P as a fitting parameter, but they did discuss (on page 3) the effect of choosing different values of P .
- ⁷⁵ In Ref. 44, Kolokolov *et al.* state that their modification of the Kane Hamiltonian has less error (measured with respect to the original Kane Hamiltonian) in the coefficient of k^4 in the secular equation than the model of Ref. 32. This

assertion is meaningless, however, since the Kane Hamiltonian is not valid to order k^4 . It should also be noted that the modification proposed in Ref. 44 is not invariant with respect to the symmetry operations of the T_d group.

⁷⁶ The conduction subband structure was not considered here because (see Fig. 1) the L conduction valleys of the model system are nearly degenerate with the Γ valley.^{50,51} Hence, a correct treatment of the conduction subbands in the model system would require the inclusion of intervalley mixing, which is beyond the scope of the Kane model. (To put this in another way, the exact conduction subbands of the LDA model system have “spurious solutions” of their own that would lead to unnecessary complications.)

⁷⁷ X. Gonze *et al.*, *Comput. Mater. Sci.* **25**, 478 (2002).

⁷⁸ X. Gonze *et al.*, *Z. Kristallogr.* **220**, 558 (2005).

⁷⁹ The ABINIT code is a common project of the Université Catholique de Louvain, Corning Incorporated, and other

contributors (URL <http://www.abinit.org>).

⁸⁰ L. Leibler, *Phys. Rev. B* **12**, 4443 (1975).

⁸¹ L. Leibler, *Phys. Rev. B* **16**, 863 (1977).

⁸² E. N. Adams and E. I. Blount, *J. Phys. Chem. Solids* **10**, 286 (1959).

⁸³ E. I. Blount, in *Solid State Physics*, edited by F. Seitz and D. Turnbull (Academic, New York, 1962), vol. 13, pp. 305–373.

⁸⁴ M. Lax, *Symmetry Principles in Solid State and Molecular Physics* (Wiley, New York, 1974).

⁸⁵ M. V. Berry, *Proc. R. Soc. Lond. A* **392**, 45 (1984).

⁸⁶ G. Sundaram and Q. Niu, *Phys. Rev. B* **59**, 14915 (1999).

⁸⁷ E. N. Adams, *Phys. Rev.* **85**, 41 (1952).

⁸⁸ The relationship is not an exact equivalence because the quasi-Bloch basis differs from a true Bloch basis and because external fields are not included here.